University of Alberta

Hydrogeological Characterization of the Red River Formation, Williston Basin, Canada-USA

By

Zsolt Margitai ©

A thesis submitted to the Faculty of Graduate Studies and Research in partial fulfillment of the requirements for the degree of Master of Science

Department of Earth and Atmospheric Sciences

Edmonton, Alberta

Fall 2002

0-612-81438-6

University of Alberta

Release Form

Name of Author: Zsolt Margitai

Title of Thesis: Hydrogeological Characterization of the Red River Formation, Williston Basin, Canada-USA

Degree: Master of Science

Year This Degree Granted: 2002

Zsolt Margitai

320 Michener Park
Edmonton, AB, Canada
T6H 4M5

Date: Apr 26, 2002

University of Alberta

Faculty of Graduate Studies and Research

The undersigned certify that they have read, and recommend to the Faculty of Graduate Studies and Research for acceptance, a thesis entitled "Hydrogeological Characterization of the Red River Formation, Williston Basin, Canada-USA" submitted by Zsolt Margitai in partial fulfillment of the requirements for the degree of Master of Science.

Ben Rostron
Dr. Ben Rostron, Supervisor

Carl Mendoza
Dr. Carl Mendoza

Hans G. Machel
Dr. Hans Machel

Dr. Walter Jones

Date: April 24, 2002

Abstract

Extensive exploration activity began in the Paleozoic section of the Williston Basin soon after the discovery of promising oil reserves in southern Saskatchewan in the mid-1990s. Significant hydrocarbon potential was indicated, and it sparked interest in the Red River Formation.

Results of the present work confirm the previously recognized three distinctive water types ($CaSO_4$, NaCl, and Na-CaCl) in the Red River Formation. Two flow regimes exist within the study area: one gravity-driven, originating from high elevations; the second, a sluggish brine, sitting in the deepest part of the basin. Freshwater hydraulic heads decrease from southwest to north-northeast; however, the presence of high-density fluids modifies the freshwater flow patterns in direction and magnitude. Application of the UVZ-method shows hydrocarbon migration towards the edges of the basin.

Acknowledgements

Thank you first to Dr. Ben Rostron, my supervisor, for your guidance and patience. Your generosity and trust opened a new world for me. Without your help I would not be here.

Thanks to my committee members, Dr. Carl Mendoza, Dr. Hans Machel, Dr. Walter Jones, for the improvement you made to the drafts.

I would like to thank Mary Bluemle, Tom Heck, Walter Jones, Kim Kreis, Richard LeFever, Mack McGillivray, Ben Rostron, the American Institute of Formation Evaluation Ltd., and the Canadian Hydrodynamics Ltd. for providing data.

Thanks to Dr. József Tóth for helping me at the beginning.

This research was possible because of the financial assistance from Dr. Rostron's NSERC grant. The Department of Earth and Atmospheric Sciences at the University of Alberta provided teaching and research assistantships. Dr. Rostron and Dr. Mendoza let me use the computer equipment. Thank you.

Dedication

For Kriszta and Lili

Table of Contents

List of Tables

List of Figures

Chapter 1 - Introduction

1.1 Historical Perspective

The beginning of groundwater hydrology dates back to 1856 when Henry Darcy described an experiment that analyzed the flow of water through sands. The result was Darcy's law. The first use of patterns of groundwater movement appeared as early as the late 19^{th}, early 20^{th} century (Slichter, 1897-98; Darton, 1905). In the 1920's, Coffin used fluid pressures to map the degree of freshwater invasion into sedimentary basins (Powley, 1990). In the ensuing years, the detailed mathematical fundamentals of groundwater flow were established (Meinzer, 1923; Dachler, 1936; Muskat, 1937; Hubbert, 1940).

The idea that hydrocarbons in a groundwater environment are impelled by the forces of buoyancy was first formulated in the mid 1860's; by the 1890's the anticlinal theory (i.e., the crests of anticlines are the primary accumulation sites for oil and gas) became dominant and went unchallenged until World War II (Powley, 1990). The only significant deviation was manifested in the works of Munn (1909), Shaw (1917), and Rich (1921), among others, representing the hydraulic theory of oil and gas accumulation. However, it was not completely accepted until Hubbert's (1953) explanation on transport and entrapment. In the past few decades, the theory of gravity-induced cross-formational flow was confirmed in deep sedimentary basins (e.g., Tóth, 1978, 1980).

1.2 Study Area

The Ordovician Red River Formation of the Williston Basin was selected for this study for a number of reasons. First, the horizon has never been investigated on a regional basis. It has been an important exploration target since the 1950's, but plenty of studies (e.g. Murray, 1959; Potter and St. Onge, 1991; Longman et al., 1998) were limited to smaller areas, fields, most likely due to local economic importance. Second, significant reserves were known from the U.S. part of the basin, while on the Canadian portion, the Red River Formation has been a minor contributor to the reserves until the mid-1990s. However, major discoveries in 1995, in southeastern Saskatchewan led to enlivened activity. Third, despite the renewed interest in the formation, an extensive dataset, consisting of rock and fluid properties necessary for a hydrogeological and petroleum hydrogeological study, has never been established. Fourth, the formation seemed suitable for identification and mapping of secondary hydrocarbon migration routes and accumulation sites under hydrodynamic conditions by using the UVZ method (Hubbert, 1953).

The project area, comprising part of the Canadian provinces of Saskatchewan and Manitoba, and the states of North Dakota, South Dakota and Montana of the United States, is restricted to that segment of the Williston Basin where the Red River Formation exists (Figures 1.1 and 4.2). The isopach contours have been determined from drilling results from Saskatchewan and Manitoba (data from Kim Kreis of Saskatchewan Energy Mines, pers. comm., 1999, and Bezys and Conley, 1998, respectively), and from existing maps from the United States (Gries, 1981; Brown et al., 1984). In the absence of data and maps in parts of Montana and Wyoming, the boundary was estimated. The area covers roughly 1,200,000 km^2.

1.3 Objectives

The present study has five main objectives. First, to acquire, organize, and prepare a dataset that may also be used by future investigations. The reason why it has not been done previously is manifold: deep well penetration was/is limited compared to shallower parts of the basin, private companies hold plenty of data and it is often difficult, time consuming and expensive to acquire them. Furthermore, many of the existing databases are not very well (or at all) organized, or not available in digital format. Second, to develop and implement a comprehensive basin-wide study not divided by political boundaries, or industrial interest. Third, to identify unique culling criteria for various parameters, which are representative of the Red River Formation. Fourth, to investigate the flow regime and its effects on hydrodynamic trapping. Fifth, to apply Hubbert's UVZ-method (Hubbert, 1953) to the formation of interest.

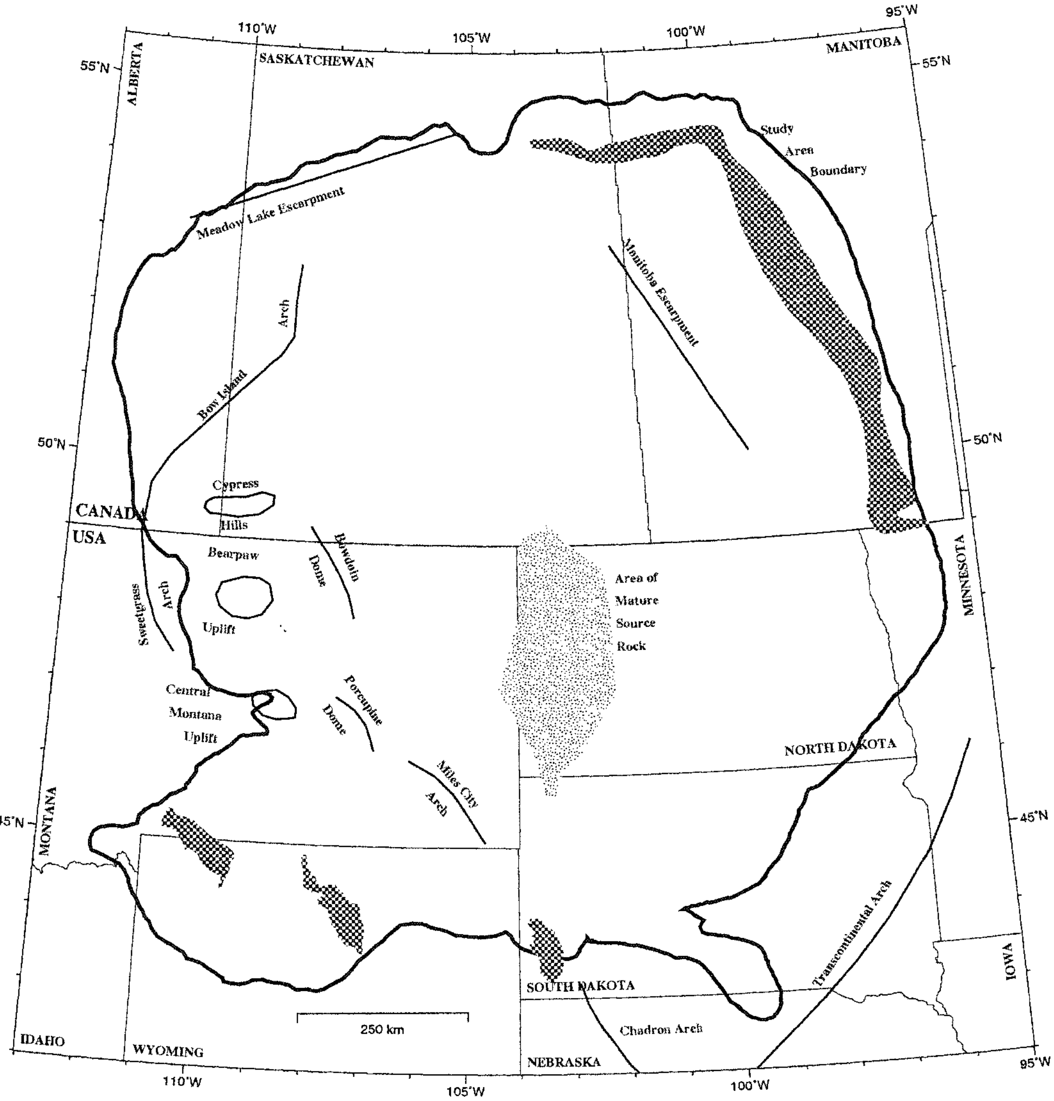

Figure 1.1 Map showing study area, physiographic features (after Bachu and Hitchon, 1996), approximate area of thermally mature Red River Formation source rock (after Martiniuk et al., 1998) and outcrops (checkered pattern, after Brown et al., 1984; and Mossop and Shetsen, 1994)

Chapter 2 - Study Area

2.1 Location of the Williston Basin

The Williston Basin is a large, elongated circular depression on the North American Craton underlying the eastern portion of the Western Canada Sedimentary Basin and the Northern Great Plains in the United States, covering several hundred thousand square kilometres across parts of Saskatchewan, Manitoba, Montana, and North and South Dakota (Figure 1.1). Laird (1956) defined the Williston Basin using the zero elevation of the Cretaceous Dakota Sandstone, which was widely accepted. However, it is not appropriate to apply the same definition to studies involving Paleozoic formations. Therefore, in this study, the basin is defined by a series of arches and uplifts, including the Transcontinental Arch, Central Montana Uplift, Sweetgrass Arch, and Meadow Lake Escarpment, while the north and northeastern sides are roughly defined by the Canadian Shield.

The area is characterized by broad plains that have been dissected by streams. Relief can reach hundreds of metres where streams have cut into the soft underlying rock. Elevations range from 2,500 m to 3,000 m on the southwestern side of the basin to less than 300 m at the Canadian Shield. A sudden change in altitude, to values greater than 2,000 m, occurs at the Montana-Wyoming border (Figure 2.1).

2.2 Geology of the Williston Basin

The geology of the Williston Basin was studied in detail (e.g., Mossop and Shetsen, 1994, Chapter 27). In summary, it is clear that the Williston Basin was an area of differential subsidence throughout much of its history. In Cambrian-Ordovician time sedimentation kept pace with subsidence, but in Mississippian and Jurassic time the subsidence rate became more rapid than the sedimentation rate. During Devonian and Cretaceous time, the basin appears to have been an inactive epeirogenic element of an extensive basinal feature (Kent, 1987).

Sedimentation in the basin is characterized by cyclical transgressions and regressions by repeated sequences of clastics and carbonates. Initial sedimentation developed over the crystalline Precambrian surface, beginning with the Sauk sequence. Rocks of the Tippecanoe sequence represent the second cycle of transgression, sedimentation and regression. By this time, the basin was a well-defined depression. During the Kaskaskia sequence, activity on the Transcontinental Arch tilted the basin northward. Terrestrial clastics with marine and evaporite sediments characterize the next sequence, the Absaroka. During Zuni time, uplift, erosion and volcanism occurred preceding the shaly sandstones, lignites and limestones of Tejas time (Gerhard et al., 1982).

The tectonic history of the Williston Basin can be divided into three main periods during which the present overall shape of the basin and its internal structure developed (Rédly, 1998). In the first, "Pre-Williston" phase a mantle intrusion resulted in radially arranged extensional fractures and faults of the crust in the center of the basin, and circumferentially arranged compressive structures at the flanks. The first Paleozoic rocks were deposited in the beginning of the second, Sauk-Absaroka intracratonic phase, resulting in the reactivation and inversion of existing structural trends. During the third, Zuni-Tejas, phase the Williston Basin became part of the Western Canada Sedimentary Basin. Compressional forces resulted in a NNW-SSE elliptical elongation of the circular basin (Rédly, 1998).

Sediments within the basin have a maximum thickness of 5 km in the USA and about 3.5 km in Canada (Gerhard et al., 1982; Mossop and Shetsen, 1994). The Phanerozoic succession comprises:

1. Paleozoic rocks, predominantly carbonates, greater than 2000 m in thickness
2. Mesozoic strata of fine terrigeneous clastics with a thickness of about 1500 m

3. Tertiary formations of 1000 m thick coarse terrigeneous clastics.

2.3 Geology of the Red River Formation

The Late Ordovician (Edenian, Maysvillian and early Richmondian in age) Red River Formation is more than 210 m thick in western North Dakota and then is truncated by Devonian erosion around the borders of the basin (Figure 2.2). Deposition of the formation may have been minimal over much of the Transcontinental Arch. (Cecile and Norford, 1993).

Red River strata were first studied in 1900 by Dowling along the west shore and islands of Lake Winnipeg (Foerste, 1929). He correlated it with the Trenton Formation of Minnesota and subdivided the sequence into three units. Later Foerste renamed the Trenton Formation to the Red River Formation (ibid.).

Previous stratigraphic works have been conducted by Baillie (1952), Andrichuk (1959), Brindle (1960), Kent (1960), Cumming (1975), and Kendall (1976). An overview of the stratigraphy of the whole region was provided by Porter and Fuller (1959). Other papers that describe the lithology, stratigraphy, and environments of deposition of the formation include: McCabe and Bannatyne (1970), Kohm and Louden (1978), Haidl et al. (1997), and Montgomery (1997).

Generally, sedimentation in the Red River Formation can be characterized by cycles. Each complete cycle begins with deposition of a fossiliferous, burrow-mottled mudstone-wackestone unit, passes through a laminated to thin bedded carbonate mudstone, and culminates in deposition of basin-centered evaporates (Kreis and Haidl, 1997).

Nomenclature of the Red River Formation is complicated, with different names in different places (Table 2.1). In North Dakota, the formation is subdivided into two informal members. The lower one is the lower two-thirds of the formation and is composed of fossiliferous and selectively dolomitized limestones. The upper member contains four porosity zones, the “D”, “C”, “B”, and “A” zones, in ascending order (Carroll, 1979). The upper three zones are capped by anhydrite while the “D” is not.

In southeast Saskatchewan, the Red River Formation is formally subdivided into an upper formation (Herald) and a lower (Yeoman) one. The Herald is further divided in ascending order into the Lake Alma and Coronach Members, and the Redvers Unit. Where this division cannot be recognized, Red River Formation is used.

In Manitoba, the formation is comprised of four members: the Dog Head, Cat Head, Selkirk and Fort Garry, in ascending order. The Fort Garry Member can be correlated with the Herald Formation of Saskatchewan, while he other three members are equivalent to the Yeoman Formation (Martiniuk et al., 1998).

Red River strata conformably overlie the shales and sandstones of the Winnipeg Formation in southern Manitoba and North Dakota. The strata rest unconformably on the Cambrian Deadwood Formation in western Saskatchewan, and on the Precambrian basement in northern Manitoba. The Red River is overlain disconformably by the shales of the Stony Mountain Formation (Table 2.1).

2.4 Hydrogeology

The Williston Basin is a classic example of a large-scale groundwater flow system (Downey et al., 1987). In a basin with sloping flanks, a pattern of groundwater flow is developed, where flow is descending, lateral, and ascending in recharge, midline, and discharge areas, respectively, relative to the water table. Topographic uplifts (e.g., Black Hills, Bighorn Mountain, Wind River Range) created recharge areas for hydrostratigraphic units of the Williston Basin (Berg et al., 1994), whereas discharge takes place along the eastern and northeastern sides.

A hydrostratigraphic unit is the basic unit of hydrogeology, which can be a single lithostratigraphic formation, or part of it, or a combination of formations, possessing similar hydraulic properties. An aquifer is defined as a saturated, permeable unit capable of transmitting significant quantities of water under normal hydraulic gradients (Freeze and Cherry, 1979). Less permeable beds, which retard the movement of water, are called aquitards.

In the U.S. portion of the basin the stratigraphic column is divided into five regional aquifers and four aquitards by Downey (1982). On the Canadian side, a more detailed classification exists with seven aquifers, five aquitards and one confining layer (aquiclude) by Bachu and Hitchon (1996). The aquifer of interest, the Cambrian-Ordovician, has been further divided into three sub-aquifers and two aquitards (Benn and Rostron, 1998). Table 2.2 summarizes the stratigraphic and hydrostratigraphic units overlying the Precambrian basement.

Bachu and Hitchon (1996) classify the aquifers into three categories: open, semi-open, and closed. Open ones (Cambrian-Ordovician, Devonian, and Manville) are exposed at the surface in both recharge and discharge areas. The Mississippian and Pennsylvanian aquifers are semi-open, since they are exposed only in recharge areas. The Viking aquifer is considered as a closed system, as it does not outcrop except for a small area in the Black Hills. A cross-section across the basin, with the hypothetical flow directions, is shown in Figure 2.3.

The Williston Basin is believed to contain two distinct flow systems. The first is an active system recharging in high elevations on the southern, southwestern edge of the basin, and discharging in the eastern Dakotas and in Manitoba in low areas. Potentiometric maps (Downey, 1984; Berg et al., 1994; Bachu and Hitchon, 1996) show the north- and northeastward, topographically driven flow toward the Canadian Shield and the eastern flank of the basin. The second regime is a system of very low groundwater flow on the eastern side of the Williston Basin (Downey, 1984) representing a sluggish brine segment whose origin is not completely understood.

The possibility of hydrodynamic conditions in the basin was first explained by Murray (1959). Regional flow patterns were established later in the 1980s (e.g., Downey, 1984). Most of the previous hydrogeological studies on the U.S. side (e.g. Downey, 1984) relate to water resources evaluation, focusing on water quality, flow rates and flow directions. Studies on the Canadian side (Potter and St. Onge, 1991; Bachu and Hitchon, 1996) have more application to petroleum geology and hydrocarbon exploration. Within the whole Williston Basin, only one study (Bachu and Hitchon, 1996) has interpreted the hydrogeology near the boundaries of this project.

Only one basin-scale hydrochemical study exists (Benn and Rostron, 1998). Other large-scale studies have been performed by the United States Geological Survey (Neuzil et al., 1982; Bredehoeft et al., 1983; Busby et al., 1995), but these do not provide any coverage north of 49° N.

2.5 Petroleum Geology

2.5.1 Historical Overview

The Williston Basin contains more than 700 oil fields (MDS Williston Basin Oil and Gas Fields Map, Minerals Diversified Services, 1998), all of which have been discovered since 1950. Even though Mississippian rocks hold the majority of the known reserves, commercial hydrocarbon has been found in rocks of all ages except Tertiary, Permian and Precambrian.

Sporadic pre-World War I exploration activity took place, but the few deeper wells drilled were unsuccessful. Shallow gas was discovered in the Upper Cretaceous Eagle Sandstone in southeastern Montana in 1916.

Following World War II, numerous companies renewed their interest in the deeper section of the basin that culminated in the 1951 discovery of the Beaver Lodge Field on the Nesson Anticline in North Dakota and the Richey Fields in eastern Montana. Early production on the Nesson Anticline was mainly from Mississippian carbonate reservoirs and on the Cedar Creek Anticline from Ordovician and Silurian carbonates.

With the strong oil price rise in the early 1970s, exploration intensified again, particularly in the Red River, and in Silurian and Devonian formations, which resulted in the beginning of production in the Minton pool of Saskatchewan in 1976.

Despite the initial success, only eight additional oil wells were completed here in the following 15 years (Haidl, 1990). The 1995 discovery of oil reserves in the Red River Formation in the Midale area of southern Saskatchewan proved the presence of reservoir horizons deeper in the basin, sparked interest and made the formation a primary target for intensive exploration. Since then more than 110 new Red River wells have been put into production in the province, compared to the 16 in the previous nearly four decades (Kreis and Kent, 2000).

2.5.2 Source and Production of Hydrocarbons

Hydrocarbons in the Williston Basin have been extensively investigated. The earliest study of Williams (1974) identified three oil families (Type I, II, III) by means of carbon isotopic and gasoline range compositions. His work was later expanded (Leenheer and Zumberge, 1987) who recognized five oil families (Group 1-5) in central Williston Basin. Finally, new discoveries in the early 90's required some reclassification (Osadetz et al., 1992) into four families (Family A, B, C, D). This model is now widely accepted over most of the basin. The correlation between the classification schemes is shown in Table 2.3. Family A oil can be found in Upper Ordovician reservoirs, Family B oils occur in Bakken Formation reservoirs, all Mississippian Madison pools and Mesozoic oil fields in southeastern Saskatchewan and southwestern Manitoba contain Family C oils, and Family D oils occur in numerous formations, including Winnipegosis pinnacle reefs and Ratcliffe Beds, Madison Group (Osadetz et al., 1992).

Oil production from the Red River Formation (in excess of 88,000,000 m^3 of oil, Martiniuk et al., 1998) is derived from the Family A oil-source system (Osadetz et al., 1992). Geochemical studies (Osadetz et al., 1992; Osadetz and Snowdon, 1995) indicate that oil produced from the Red River Formation in Saskatchewan is sourced from kukersitic beds in Ordovician carbonates in Saskatchewan, North Dakota and Montana. Kukersites are kerogenous lime mudstones with Gloeocapsomorpha prisca alginite (Osadetz et al., 1992). Numerical modelling suggests that these kukersites, which are the richest in the basin in terms of initial petroleum potential, have generated a much larger volume of oil than that yet discovered (Burrus et al., 1995). Red River Formation sources first entered the oil window at the end of Cretaceous time, and reached peak generation about 75 million years ago (ibid).

In North Dakota and Montana the “C” and “B” units are productive. In Saskatchewan, production is from the upper part of the Yeoman Formation and from the lower part of the Herald (Lake Alma Member) Formation. Oil staining has been found in cuttings and cores in southwestern Manitoba (Martiniuk and Barchyn, 1994) but no production has been reported yet. Burrow-mottled, fossiliferous lime wackestones and dolomitic limestones have been identified as existing and potential reservoirs within the formation.

Most of the oil production has occurred close to the area of thermally mature source rock (Figure 1.1). However, the existence of Red River Formation production outside that area (e.g., Minton pool in Saskatchewan (Potter and St. Onge, 1991), Lantry Field in South Dakota (Longman, 1998)) provides evidence of long distance migration from areas of thermal maturation.

Data on existing pools indicate that structure has an important role on oil entrapment. Although structural closure is the dominant trapping mechanism, most of the pools are combination traps. Furthermore, potential hydrodynamic trapping might have played an important role in the mechanism but has not been exhaustively investigated yet.

A number of published studies which deal with hydrodynamics or migration of hydrocarbons range in scope from size of a field or part of a province/state (Potter and St. Onge, 1991; Martiniuk and Barchyn, 1994; Longman et al., 1998; Martiniuk et al., 1998) to those of more extensive areas of the basin (Burrus et al., 1996; Li et al., 1998a; Li et al., 1998b; Obermayer et al., 1998; Osadetz et al., 1998).

	Montana North Dakota		Saskatchewan			Manitoba	
SILURIAN	Stonewall Formation		Stonewall Formation			Stonewall Formation	
ORDOVICIAN	Stony Mountain Formation	Gunton Member	Stony Mountain Formation	Gunton Member		Stony Mountain Formation	Gunton Member
		Gunn Member		Gunn Member / Hartaven Member			Gunn Member
	Red River Formation						
		"A" anhydrite	Red River Formation	Herald Formation	Redvers Unit	Red River Formation	Fort Garry Member
		"B" anhydrite			Coronach Anhydrite		
		"B" laminated			Coronach Member		
		"B" burrowed					
		"C" anhydrite			Lake Alma Anhydrite		
		"C" laminated			Lake Alma Member		
		"C" burrowed		Yeoman Formation			Selkirk Member
		"D"					Cat Head Member
							Dog Head Member
	Winnipeg Formation		Winnipeg Formation			Winnipeg Formation	

Table 2.1 Generalized stratigraphy of the Lower Paleozoic section, Williston Basin (after Martiniuk et al. 1998)

Age[1]	System		Stratigraphy USA[2]	Stratigraphy Canada[2]	Hydrostratigraphy USA[3]	Hydrostratigraphy Canada[4]
1.6	Quaternary		Laurentide Drift	Laurentide Drift	Tertiary/Upper Cretaceous Aquifer	Upper Aquifer System
	Tertiary		Golden Valley Fm.			
66.4			Fort Union Fm.	Ravenscrag Fm.		
	Cretaceous	U	Montana Group	Montana Group	Cretaceous Aquitard	Cretaceous Aquitard System
		U	Colorado Group	Colorado Group	Lower Cretaceous Aquifer	Viking Aquifer
						Joli Fou Aquitard
		L	Dakota Group	Mannville Group		Mannville Aquifer
144		L				
	Jurassic	U	Swift Fm.	Rierdon/Swift/Vanguard Fms.	Jurassic Aquitard	
		M	Rierdon Fm.	Gravelbourg/Piper/Shaunavon Fms.		Mississippian-Jurassic Aquitard System
		M	Piper Fm.			
208		L		Amaranth/Watrous Fms.		
	Triassic	U				
		M		Lower Amaranth/Red Beds/Lower Watrous Fms.		
245		L				
	Permian		Spearfish Fm.			
			Minnekahta Fm.			
286			Opeche Fm.			
	Pennsylvanian		Minnelusa Fm.		Pennsylvanian Aquifer	
			Amsden Fm.			
320			Tyler Fm.			
	Mississippian	U	Otter Fm.		Mississippian Aquitard	
		U	Kibbey Fm.	Kibbey Fm.		
			Charles Fm.	Charles/Midale/Poplar/Ratcliffe Fms.		
		L	Mission Canyon Fm.	Alida/Frobisher/Mission Canyon/Tilston Fms.	Madison Aquifer	Mississippian Aquifer
360		L	Lodgepole Fm.	Lodgepole/Souris Valley Fms.		
			Bakken Fm.	Bakken Fm.	Devonian Aquitard	Bakken Aquitard
	Devonian	U	Torquay Fm.	Three Forks Fm.		Devonian Aquifer
		U	Birdbear Fm.	Birdbear Fm.		
		U	Duperow Fm.	Duperow Fm.		
		M	Souris River Fm.	Souris River Fm.		
		M	Dawson Bay Fm.	Dawson Bay Fm.		
		M	Prairie Fm.	Prairie Fm.		Prairie Aquiclude
		M	Winnipegosis Fm.	Winnipegosis Fm.		Winnipegosis Aquifer
		M	Ashern Fm.	Ashern Fm.		Silurian-Devonian Aquitard
408		L				
	Silurian		Interlake Fm.	Interlake Fm.		
438			Stonewall Fm.	Stonewall Fm.		
	Ordovician	U	Stony Mountain Fm.	Stony Mountain Fm.	Cambrian-Ordovician Aquifer	Basal Aquifer System
		M	Red River Fm.	Red River Fm.		
		M	Winnipeg Fm.	Winnipeg Fm.		
505		L				
	Cambrian	U	Deadwood Fm.	Deadwood Fm.		
		M				
570		L				
	Precambrian				Basement	Basement

Notes:

1 Age in million years
2 Stratigraphy based on the Western Atlas Canada Ltd. Correlation chart
3 Based on Downey et al., 1987
4 Based on Bachu and Hitchon, 1996
- - - - - - - - - Unconformity

Table 2.2 Generalized stratigraphy and hydrostratigraphy of the Williston Basin

<table>
<tr><th>Classification 1
Williams (1974)</th><th>Classification 2
Leenheer and Zumberge (1987)</th><th>Classification 3
Osadetz et al. (1992)</th></tr>
<tr><td rowspan="2">Type I</td><td>Group 1</td><td>Family A</td></tr>
<tr><td rowspan="2">Group 3
Group 4</td><td rowspan="2">Family D</td></tr>
<tr><td rowspan="2">Type II</td></tr>
<tr><td>Group 2</td><td>Family B
Family C</td></tr>
<tr><td>Type III</td><td>Not examined</td><td>Not examined</td></tr>
<tr><td>Not examined</td><td>Group 5</td><td>Not examined</td></tr>
</table>

Table 2.3 Oil family classification schemes in the Williston Basin (after Osadetz et al., 1992)

Figure 2.1 Map of ground surface topography. Data from F. Achour (written communication, 2001). C.I. = variable (m.a.s.l.)

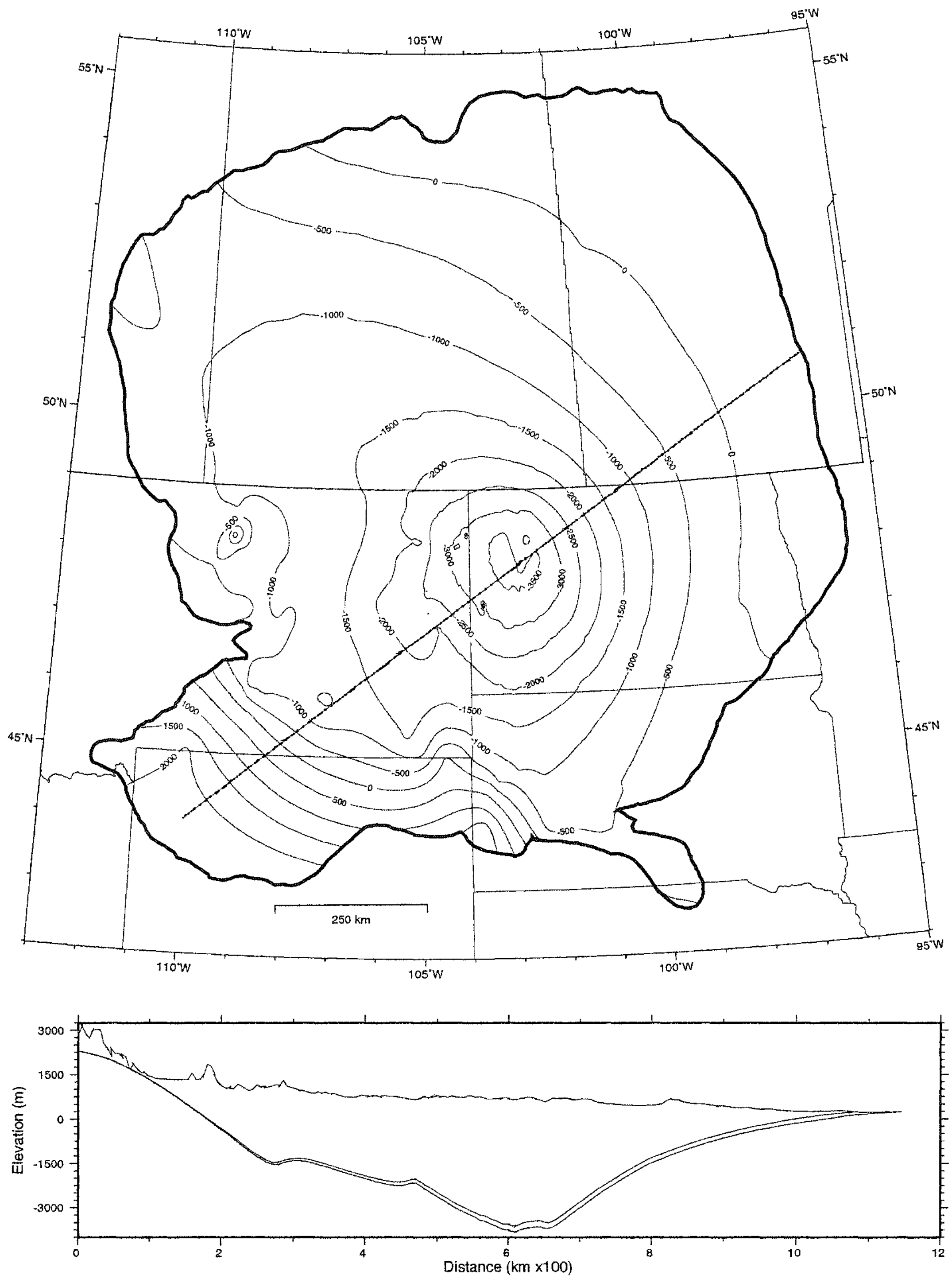

Figure 2.2 Cross-section of the Williston basin along a SW-NE trend line. Above: Red River Formation isopach map is shown.

Below: Ground surface, Red River Formation top and bottom are shown.

Cross-section across the Williston Basin

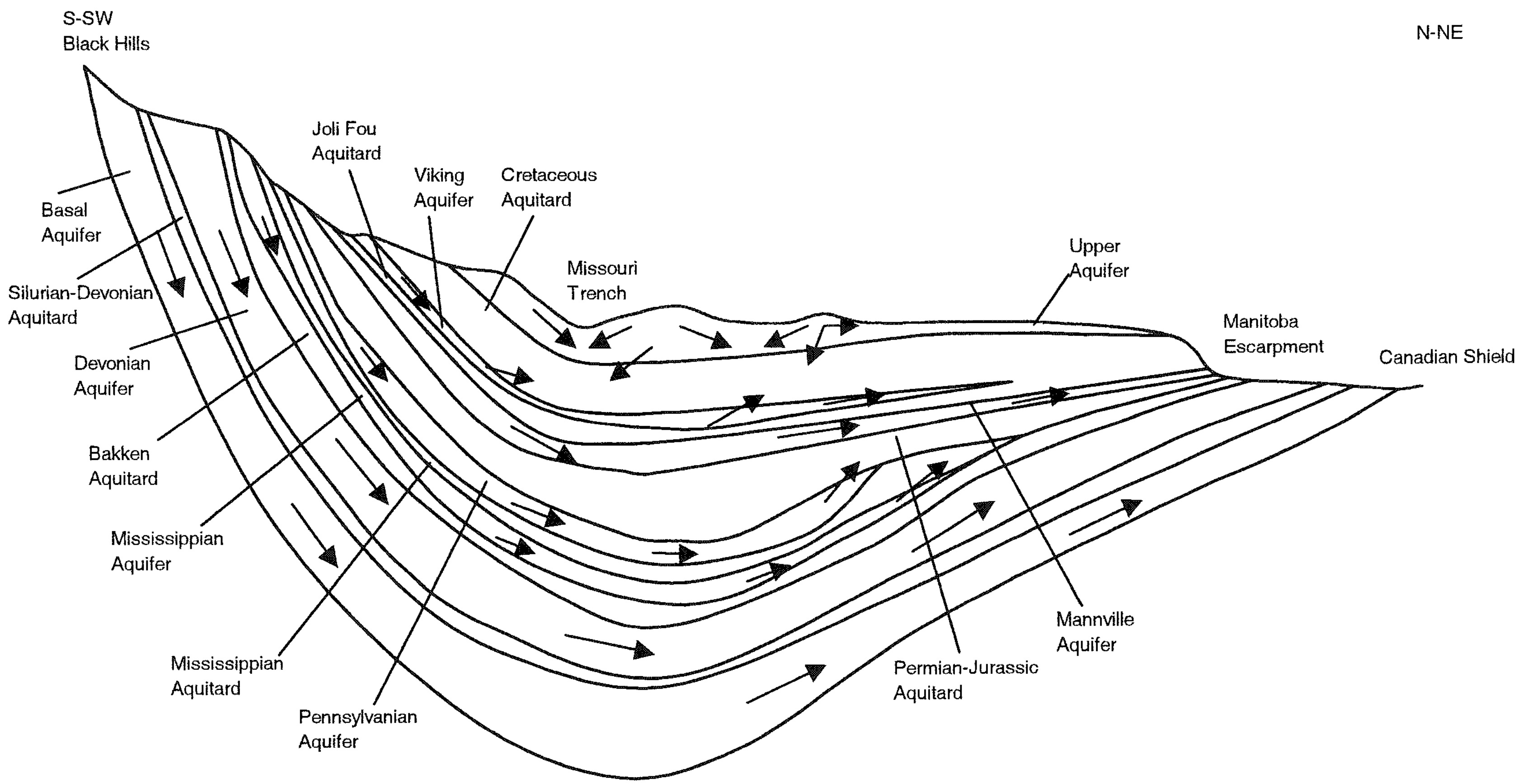

Figure 2.3 Generalized cross-section showing the north- northeastward flow of formation waters in the Williston Basin (after Bachu and Hitchon, 1996)

Chapter 3 - Fundamentals of Fluid Movement

Basic concepts relevant to the present work must be introduced to understand and determine the motion of water through a porous medium. The direction of flow in a domain, determined by the mechanical energy of a unit mass of fluid, the fluid potential (Φ), is away from regions characterized by high potentials towards regions where it is lower. Φ (L^2/T^2) can be written as the sum of three components, the potential, kinetic and elastic energies (Hubbert, 1940):

$$\Phi = gz + \int_{p_0}^{p} \frac{dp}{\rho} + \frac{v^2}{2} \tag{3.1}$$

where g is the acceleration due to gravity (L/T^2)

z is the elevation above a datum (L)

ρ is the fluid density (M/L^3)

p is the fluid pressure (M/LT^2)

p_0 is the atmospheric pressure (M/LT^2)

v is the flow velocity (L/T).

For groundwater flow, velocities are usually low, so the third term on the right hand side of the equation can be neglected. For incompressible and homogeneous fluids, $\rho = const.$, therefore equation (3.1) reduces to

$$\Phi = gz + \frac{p - p_0}{\rho} \tag{3.2}$$

Assuming constant density, at any point in a flow system the pressure can be determined by the height of the fluid column above the point and is given by

$$p = \rho g(h - z) + p_0 \tag{3.3}$$

where h, the equivalent freshwater hydraulic head is the elevation above datum to which the water will rise in an open pipe sunk to a depth of interest.

By substituting (3.3) into (3.2)

$$\Phi = gh \tag{3.4}$$

is obtained. Since the hydraulic head is directly measurable, it is a suitable expression for the potential.

The force, E, which drives groundwater flow, is the total force per unit of mass (Hubbert, 1940), and equals the vectorial sum of the gravitational ($\vec{E}_{grav}$) and pressure ($\vec{E}_{pres}$) forces:

$$\vec{E} = -grad\,\Phi = \vec{E}_{grav} + \vec{E}_{pres} \tag{3.5}$$

By substituting (3.2) into (3.5) gives

$$-\,grad\,\Phi = -grad(gz) - \frac{1}{\rho}\,grad\,p \tag{3.6}$$

The gravity force can be considered constant in magnitude, and its direction is always downward; the pressure force, however, may have any direction and magnitude.

The driving force can thus be expressed in terms of the freshwater hydraulic head gradient by substituting (3.4) into (3.6):

$$-\,grad\,h = -grad\,z - \frac{1}{\rho g}\,grad\,p \tag{3.7}$$

The use of the gradient of hydraulic head as the driving force for flow is not valid for variable density (ρ_w) fluids. In such systems the buoyant force, directed vertically upward, acting on a fluid particle of density ρ_w, imbedded in a fluid of reference density (i.e., freshwater), ρ, cannot be neglected (Davies, 1987). The buoyant force is given as

$$\vec{E}_{buoy} = -grad(gz) * (\rho_w - \rho) \tag{3.8}$$

By a series of substitutions (Barson, 1993), the buoyancy-modified force (F) can be written as

$$F = -grad\,h - grad\,z * (\frac{\rho_w - \rho}{\rho}) \tag{3.9}$$

where the first term represents the equivalent freshwater head gradient, the second one is the buoyant force. According to Davis (1987) and Bear (1972), if

$$Driving\ Force\,Ratio\,(DFR) = (\frac{\rho_w - \rho}{\rho}) * \frac{grad\,z}{grad\,h} >> 1 \tag{3.10}$$

the flow is determined by the buoyancy force. When $DFR << 1$, the flow is governed by external head gradients. Davies (1987) determined that at the threshold of $DFR = 0.5$ the buoyant force became significant in a New Mexico study area.

Chapter 4 - Sources of Data, Culling Techniques

One of the goals of the thesis is to complete a regional scale study of hydrogeology in the Williston Basin. To achieve this goal a previously non-existent database, covering the whole basin, had to be created. Many factors contributed to the previous lack of truly regional coverage, among them are:

- limited deep well penetration
- multiple difficulties in obtaining data from private companies
- poor organization of existing data.

A set of basin-wide data for the Red River Formation was not available due to the large scale, and jurisdictional boundaries, i.e., the border between Canada and the United States. Most of the previous investigations had been limited by country/provincial/state lines making it impossible to see natural processes undivided.

This chapter introduces the data that were required and how they were processed to obtain a unique dataset characteristic to a selected horizon in a sedimentary basin. Also, sources and culling techniques are presented.

4.1 Sources of Data

4.1.1 Geological Data

Formation top elevations from oil and gas wells, water wells, have been filed with, and are available from, various government agencies, including: Manitoba Energy and Mines, Saskatchewan Energy Mines, Alberta Geological Survey, Oil and

Gas Division of North Dakota Industrial Commission, Montana Board of Oil and Gas Conservation (online data system), and a South Dakota Geological Survey paper (Gries, 1981). Distribution of datapoints (5259 picks) was uneven throughout the basin (Figure 4.1).

Due to the large number of points and lack of geophysical well logs, each one could not be verified. However, those that were checked proved correct. For certain areas, tops were crosschecked for accuracy by using more than one source (for Saskatchewan – Western Canada Sedimentary Basin Atlas data and Saskatchewan Energy Mines tops; for Manitoba – Western Canada Sedimentary Basin Atlas data and Manitoba Energy and Mines values). The double-checked data were consistent and reliable.

Owing to the fewer number of wells penetrating the underlying formation(s), compared to the Red River Formation, only 1874 isopach data points were available. The extent of the formation could be drawn easily in Canada on account of the abundance of wells near the zero edge. In the U.S., maps of previous studies (United States Geological Survey Professional Paper, 1984; Meyer, 1984) were used where control point coordinates were not available in spite of the best efforts to obtain them. Datapoints are well spread over the study area (Figure 4.2).

4.1.2 Water Chemistry

Numerous sources provided water analyses; however, the majority was supplied by provincial/state agencies, e.g., Saskatchewan Energy Mines, Montana Bureau of Mines, North Dakota Geological Survey. Other companies, individuals and publications, e.g., Geofluids database by Rakhit Petroleum Consulting Ltd., Manitoba Energy and Mines, Montana Geological Society Oil and Gas Fields Symposium volumes, HydroPetroleum Canada Ltd., and unpublished data (Rostron and Kreis, pers. comm.) also contributed to make the coverage as full as possible. With a few exceptions, complete analyses were available for the Red River Formation. Samples were mainly available from southeastern Saskatchewan, eastern Montana and western North Dakota.

In sedimentary basins with hundreds of water analyses it is indispensable to develop and use culling criteria to avoid utilization of incomplete and erroneous data (Hitchon and Brulotte, 1994). There are widely accepted and applied general flags to mark and remove contaminated data that are not representative of the formation water. On the other hand, every scientist needs to create his/her own detailed rules to characterize the basin, area, formation, or other smaller unit of interest.

For the study area, 2,184 analyses were available, all of them in digital format. Initial culling removed 1,751 analyses that were duplications, multiple well samples and incomplete analyses. A few records contained values of constituents that appeared unreasonable in comparison with other constituent values or for data for nearby wells; these data were discarded. In case of duplicate records, a few slight differences in the data were found, such as chemical concentrations rounded to different numbers, mistyped numbers, incorrect depth entered, misplaced decimal points, miscalculation of computed values (e.g., TDS), and incorrect location(s). In several cases, the erroneous record could not be determined, hence was deleted. Otherwise, the corrected data were left in the database because the rest of the values appeared correct and provided useful information for the study.

For the remaining 433 samples, numerical selection by comparing various parameters was made. The ten different criteria used for the culling process is explained below (1-10), and outlined in Table 4.1. However, samples with one single anomalous value were not removed automatically, but were treated with careful attention. The reason is that the erroneous value might have been derived from incautious sampling or laboratory techniques.

1. The accuracy of water analyses can be obtained by calculating the charge balance error, to make sure the data are reliable. If large ($> \pm 5 to 15\%$) deviation from equality of positively and negatively charged constituents occurs, then the record was flagged and retained for future consideration. The charge balance error (E) is expressed in the form (Freeze and Cherry, 1979):

$$E = \frac{\sum zm_c - \sum zm_a}{\sum zm_c + \sum zm_a} * 100$$

where z is the ionic valance

m_c is the molality of cation species

m_a is the molality of anion species.

All analyses in this study with $E > \pm 5\%$ were flagged.

2. Contamination of formation waters can excellently be reflected in the pH. I used pH>8 to screen records with possible mud filtrate, and pH<5 as an indication of acid wash.

3. Any small amount of OH^- reported resulted in the rejection of a record indicating acid wash. Measured values range from 0 to 400 mg/l.

4. Analyses are flagged if carbonate-ion is reported indicating mud filtrate contamination or poor sampling techniques.

5. The next flag is used when the density of the sample is less than 1000 kg/m^3. The reason can be either poor determination or presence of organic matter.

6. Analyses with high Fe-content are most likely to be subject to drill pipe corrosion contamination. After having reviewed the dataset, 15 mg/l of Fe was established as the upper limit for acceptable records.

7. Samples from mud pits, mud tanks, and from top of the fluid column were flagged and considered to be suspect.

8. Where more than one formation was reported and/or no sampling interval was given, the analysis was flagged.

9. Formation waters which are contaminated by KCl mud and for which values of K and Na are available can be culled using threshold values of K/Na specific to a given unit (Hitchon and Brulotte, 1994). Since there has not been previous value set up for the Red River Formation of the Williston Basin, based on 470 analyses K/Na>0.2 has been found to indicate severe contamination.

10. Other considerations: an additional 37 tests were discarded based on comparisons of distribution of Total Dissolved Solids (TDS) and individual ions on contour maps and Piper-diagrams.

Application of the before mentioned criteria resulted in the rejection of 1832 records, 83.9% of the original dataset.

4.1.3 Temperature

The most common source of deep subsurface temperature data is bottomhole temperatures (BHTs) recorded during geophysical logging. Unfortunately, getting an accurate temperature is not of primary importance of the logging procedure, therefore the accuracy of the readings is debatable (Barson, 1993). Moreover, the logs are usually taken only a few hours after drilling has stopped, therefore the measured temperatures are lower than the real formation temperatures due to the cooling effect of the drilling mud in deep wells (Gretener, 1981). Over the past few decades, several methods had been developed to correct the raw measurement (Hermanrud, 1986). Some of them require the knowledge of parameters (thermal conductivities and heat capacities of the mud and the strata) that are often not available. Previous publications (Majorowicz et al., 1986; Barson, 1993) use the modified Horner-method, originally applied to extrapolate pressure build-up values to true formation pressures (Horner, 1951). The thermal disturbance of the drilling may be removed if the time of end of circulation, and time of temperature measurement are known for a series of measurements.

Temperature measurements (total of 2,768) are abundant along the Montana-North Dakota state border (Figure 4.3). Two-thirds of the values were obtained from state geological surveys. Other sources include Richard LeFever of the University of North Dakota, and Walter Jones of the University of Alberta.

Unfortunately, usually only a small fraction of logs has the necessary multiple values and additional time information. However, the majority of the DST temperatures (2694) reportedly were corrected. The rest of the measurements (74) were deleted due to unreliability.

4.1.4 Fluid Densities

A few sources (Geofluids database by Rakhit Petroleum Consulting Ltd., Montana Bureau and Mines, Ben Rostron's unpublished data, North Dakota Geological Survey's online catalog of water densities and oil analyses, Annual Review by Montana Bureau of Mines) provided a very limited number of oil (424) and water (230) densities (Figure 4.4) which were unevenly scattered across the area. Contouring of oil densities was not possible owing to distribution of control points over a small area.

Drill stem tests can provide the most reliable formation water samples (Gretener, 1981). Fortunately, an adequate number of densities, among other properties, derive from DST's for the present study. Since mud filtrate is the first fluid to enter the pipe during tests, waters at the top of the column were discarded. Samples taken from the base of the column with high recovery of water were favoured. All densities below 1000 kg/m^3 were deleted due to a possible error during analysis.

Oil density values were provided in 'not corrected to reservoir conditions' form, therefore further manipulation was necessary. For those, where values were given in API gravity, the following conversion was used (England et al., 1987):

$$\rho_{oil} = \frac{141500}{API^0 + 131.5}$$

where ρ_{oil} is the density of the oil, in kg/m^3.

The chemical and physical properties of petroleum under subsurface conditions differ from those at standard pressure-temperature conditions. Oil density in the reservoir, among other properties, is affected by pressure and temperature. A method described by England et al. (1987) was used to estimate subsurface values. The correlation is based on laboratory experiments and accurate enough for the purpose of this study. The greatest compositional influence on density is the presence of lighter hydrocarbons, which is expressed as the gas-oil ratio (GOR). Knowing the oil formation volume factor (B_0) and the density at the surface (ρ_{oil}^{STP}), the density in the reservoir (ρ_{oil}) can be calculated by the following equation (England et al., 1987):

$$\rho_{oil} = \frac{(1+GOR)}{B_0}\rho_{oil}^{STP}$$

Using the data from eight Saskatchewan pools (Chris Gilboy of the Saskatchewan Energy Mines, written communication, 2001); a mean of 1.2 has been obtained for B_0. By averaging 1,763 monthly oil and gas production data, a GOR of 0.0009495 kg/kg was set up for the Red River Formation.

4.1.5 Production

Production data (102 Saskatchewan, 400 Montana and 722 North Dakota wells; 1224 total) were obtained in either digital (Saskatchewan – from the International Datashare Corporation (GeoOffice software, version 3.0, 2000); Montana – from the Montana Board of Oil and Gas Conservation (MBOGC) online database, 2000; North Dakota – from the North Dakota Industrial Commission (NDIC) Oil and Gas Division) or hard copy (North Dakota) form. All of the sources provide production dates, elevations (KB, ground) and depth of perforation. South Dakota production was not taken into account due to missing latitude, longitude coordinates and the possible error resulting from the conversion of the given township, range coordinates (occasionally sections and/or quarters were not given). Locations of production wells are shown in Figure 4.5.

The beginning of the production and the well location had to be known to be able to determine the influence of production-induced drawdown on DST pressures. Saskatchewan and North Dakota locations and dates had been tracked since the 1950s. South Dakota production had to be omitted because of the imprecision of well locations. In Montana, MBOGC does not have complete Red River production for individual wells before 1986 (Tom Richmond of MBOGC, written communication, 2000). In the early 1980s production was reported by lease and was not reliably allocated to the production formation if more than one formation produced on a lease. Furthermore, the Siluro-Ordovician was interpreted to be a common source of supply in the earliest units formed on the Cedar Creek Anticline, and production has historically been filed under that combined formation designation. Many wells have been commingled in the various formations that comprise this interval, and tracking of production at a more detailed level is not possible.

4.1.6 Pressure

885 extrapolated pressures from Drill Stem Tests (DST's) were provided for this study by Canadian Hydrodynamics Ltd., Richard LeFever of the University of North Dakota, Montana Geological Society Oil and Gas Fields Symposium volumes, and the American Institute of Formation Evaluation Ltd. (AIFE). Locations of datapoints are plotted in Figure 4.6.

Drill stem tests provide pressure data essential to any fluid flow study. The drill stem test is a procedure by which temporary completion of a well allows formation fluids to be sampled and formation pressures to be measured. Tests rarely run long enough for pressure to reach the virgin, undisturbed state, therefore a widely accepted and used graphical solution, the Horner-method (Horner, 1951) is applied to get extrapolated, representative values. Specialized companies (such as the AIFE) evaluate the tests, and assign a code (A to G) based on quality, A being of the highest one (Barson, 1993).

All pressures obtained from companies and individuals were extrapolated, and did not have to be corrected. Verification by recalculation/plotting was impossible as a result of missing build-up pressures. Table 4.2 summarizes the original and used tests by sources and regions. Sources provided of variable tests (code A through G). The E, F, and G code ones (misrun, no pressure obtained, difference in shut-in pressures, pressures build too rapidly to extrapolate with accuracy) were eliminated. The remaining DST's were further screened based on fluid recovery. Altogether 885 acceptable quality tests were retained for the study area.

4.1.6.1 Production Induced Drawdown (PID)

The stable formation pressures were examined to evaluate the possible drawdown effects due to oil production from nearby wells. One approach is to eliminate all DST's that had production wells within a certain radius from the DST test well. This way possible valid data might be eliminated. To evaluate to what degree a DST is disturbed, a computer program was used (Rostron, 1994). It calculates the distances between DST's and surrounding production wells, and indicates those ones that have production wells within 2, 5, 10, and 50 km radii. The program also computes the distance of the closest production well. Based on this distance, an area or formation characteristic number can be chosen beyond which all pressures are considered undisturbed.

A modified program (Wilkinson, 1995) calculates not only the distance, but also the time difference between those production wells that pre-date the DST. Any production wells that post-date DST's do not have any influence on the true formation pressures. The interference index (I), introduced by Tóth and Corbet (1986) uses the previously mentioned production time (t) prior to the DST (in years), and the distance (r) between the production and DST wells (in miles):

$$I = \log_{10} \frac{t}{r^2}$$

Therefore, a lower production time and higher inter-well radius result in a lower interference index indicating a possible non-disturbed test.

4.2 Contouring and Coordinate Conversion

All maps and the cross-section were created using the Generic Mapping Tools (GMT) developed by Wessel and Smith (1991). GMT is a collection of Unix tools that allows x,y or x,y,z datasets to be manipulated (filtering, gridding, projecting, etc.) The gridded values can then be contoured by the "grdcontour" program. In case of vector fields, "grdvector" reads two 2-D gridded files that represent the x and y component of a vector field and produces a plot by drawing vectors with orientation and length according to the information in the files (Wessel and Smith, 1995).

Computer contouring is less reliable than hand drawing when data are sporadic. Therefore, for some maps, fictitious data points were added to get the result that may better represent the area.

When latitudes and longitudes were not provided, the township-range-section locations were converted using programs by Lepard (1994) and Wefald (1995) for Canadian and U.S. wells, respectively.

Indicator	Reason For Rejection	Observed Values	Accepted Values/Properties
Charge balance error	Analytical error of ion balance	-91.28% to 81.64%	<5% and >-5%
pH	Mud filtrate, acid wash contamination	1.2-11.7	5 to 8
Hydroxid-ion content	Acid wash contamination	0-400 mg/l	0 mg/l
Carbonate-ion content	Mud filtrate contamination	0-21457 mg/l	0 mg/l
Density	Presence of organic matter or poor analysis	985-1278 kg/m3	>1000 kg/m3
Iron-ion content	Corrosion contamination	0-2150 mg/l	<15 mg/l
Sample location	Recovered fluid is not the formation fluid	N/A	Other than mud tank, mud pit, or top of fluid column
Multiple formations	More than one formation tested	N/A	One formation tested
K/Na ratio	KCl mud contaminaton	0-2.35	K/Na<0.2
Manual examination, graphical comparision of composition	N/A	N/A	N/A

Table 4.1 Summary of culling criteria for water chemistry analyses

		Code A	Code B	Code C	Code D	Code E	Code F	Code G	Total	Culled
Manitoba[1]	Original	7	0	0	0	0	0	0	7	
	Final (culled)	5	0	0	0	0	0	0	5	5
Saskatchewan[2]	Original	157	0	0	0	0	0	0	157	
	Final (culled)	108	0	0	0	0	0	0	108	108
Saskatchewan[3]	Original	67	0	0	0	0	0	0	67	
	Final (culled)	38	0	0	0	0	0	0	38	38
Montana[4]	Original	35	85	251	429	27	438	234	1499	
	Final (culled)	33	69	190	221	0	0	0	513	513
Montana[5]	Original	47				0	0	0	47	
	Final (culled)	47				0	0	0	47	47
North Dakota[6]	Original	226	0	0	0	236			462	
	Final (culled)	168	0	0	0	0			168	168
Other[7]		6				0	0	0	6	6
										885

Notes (sources):

1 Canadian Hydrodynamics Ltd.
2 Ben Rostron of the University of Alberta
3 Canadian Hydrodynamics Ltd.
4 American Institute of Formation Evaluation
5 Montana Oil and Gas Fields Symposium, Vol. 1-2, 1985.
6 Richard LeFever of the University of North Dakota
7 Pressures at outcrop locations

Table 4.2 Summary of pressure data by sources and locations

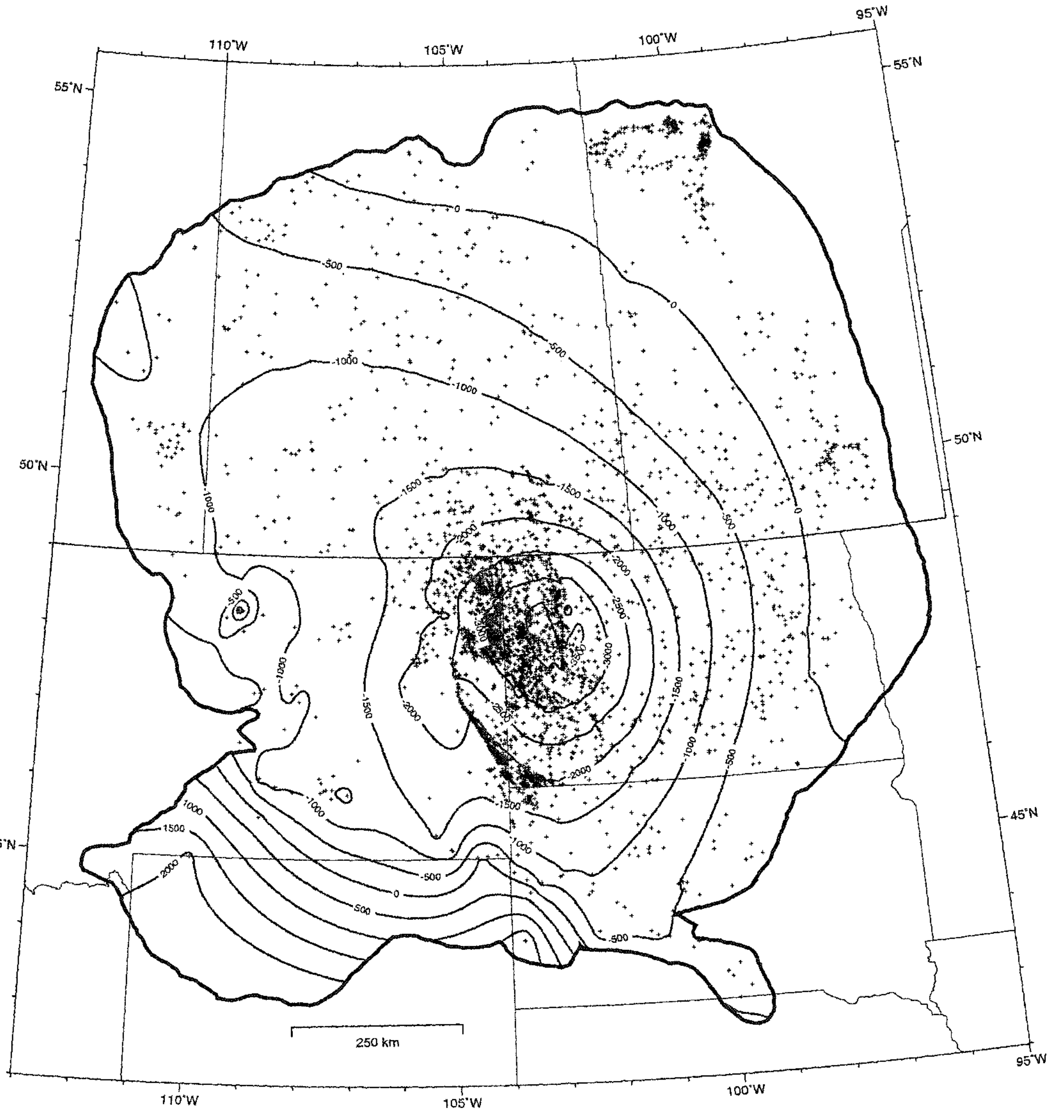

Figure 4.1 Structure contours on top of the Red River Formation (C.I.= 500 m)

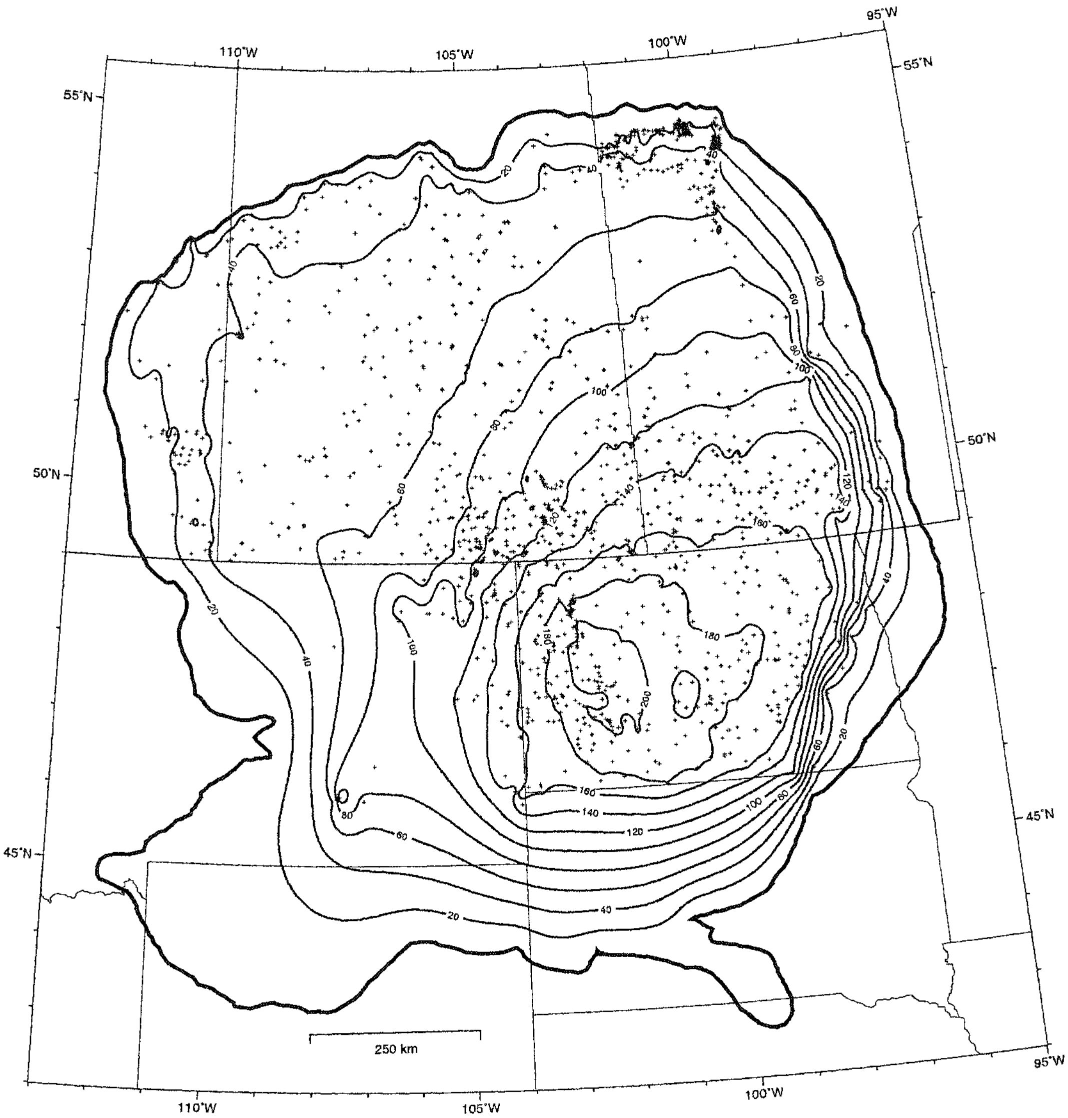

Figure 4.2 Isopach of the Red River Formation (C.I. = 20 m)

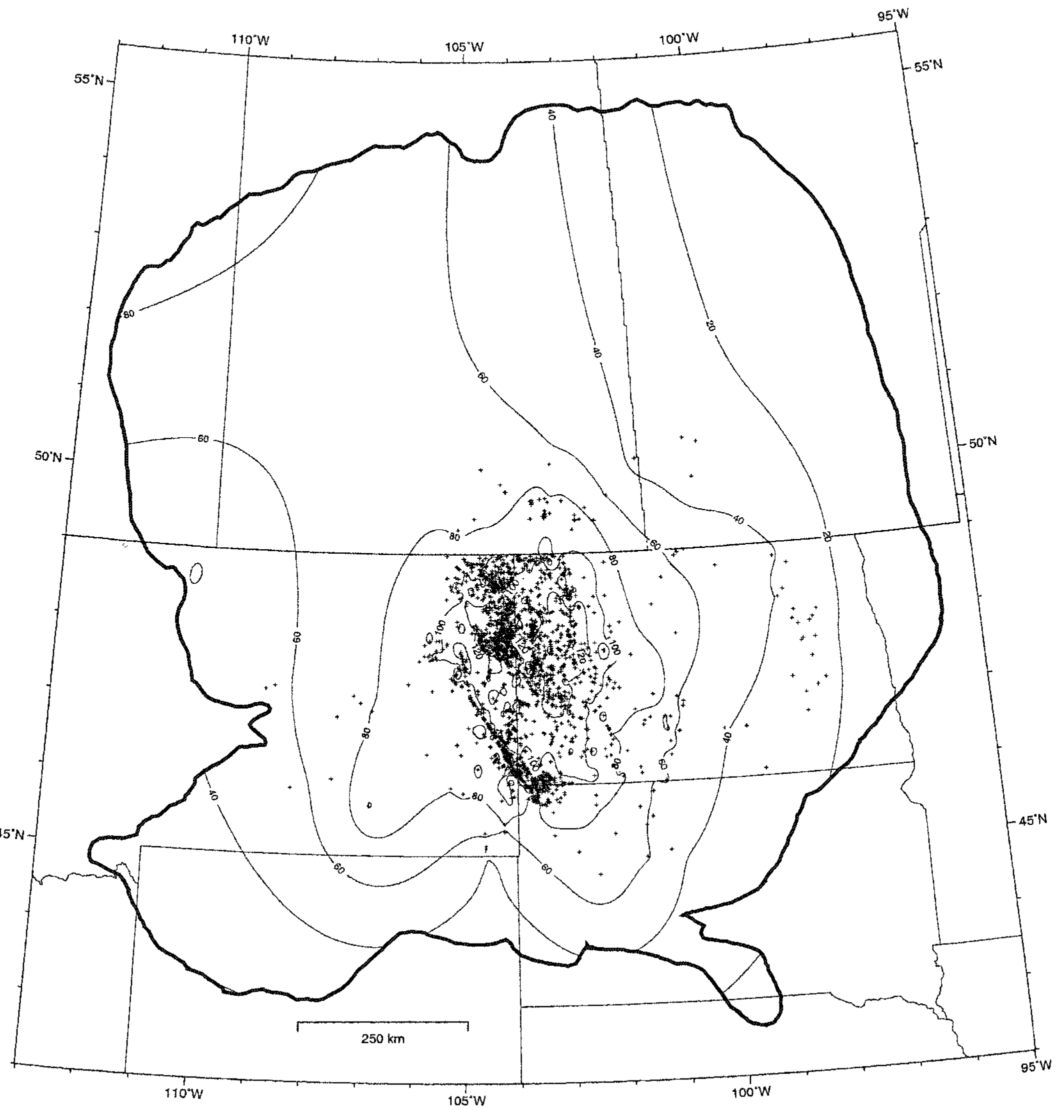

Figure 4.3 Temperature Distribution of the Red River Formation (C.I. = 20 C)

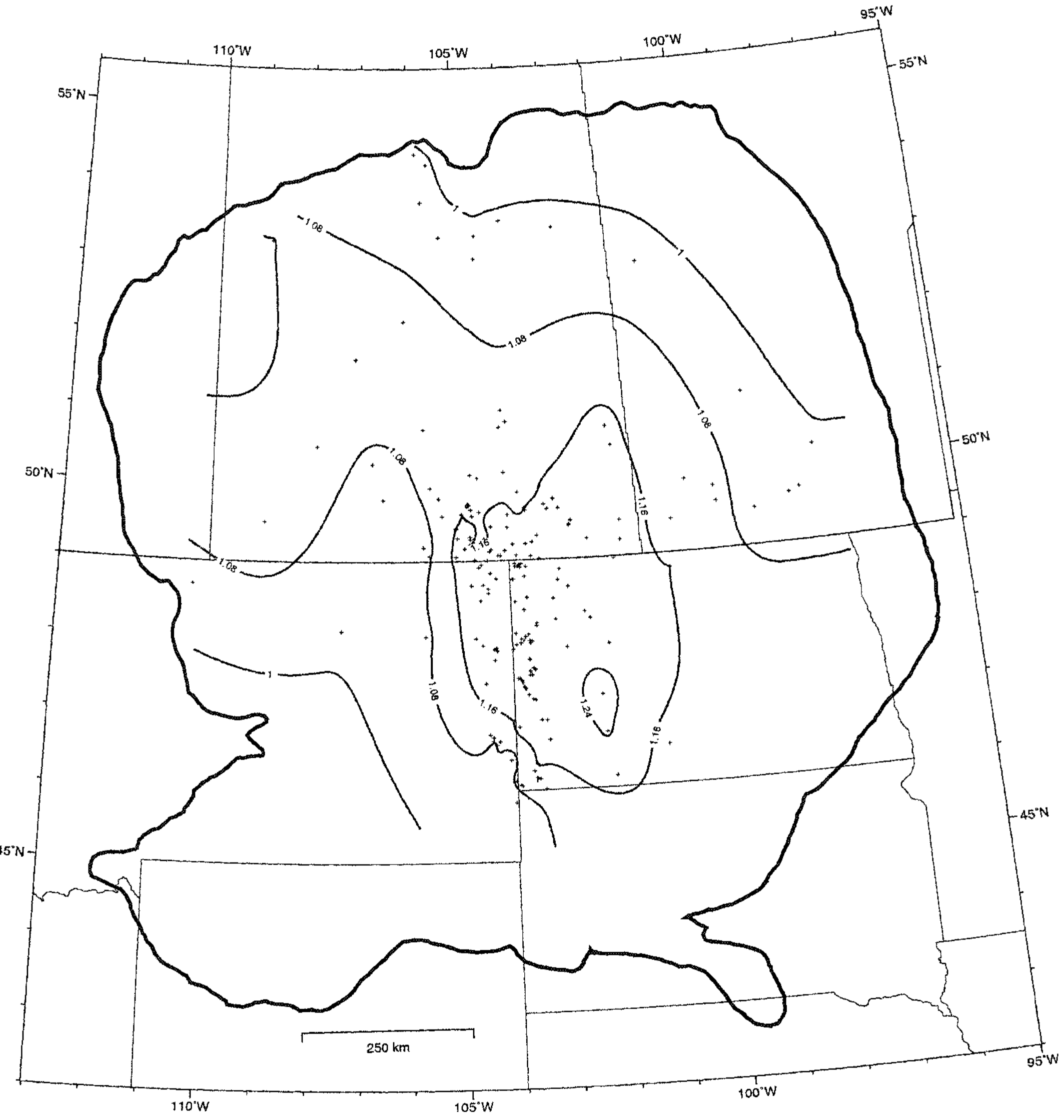

Figure 4.4 Water Density in the Red River Formation (C.I. = 0.08 g/cm³)

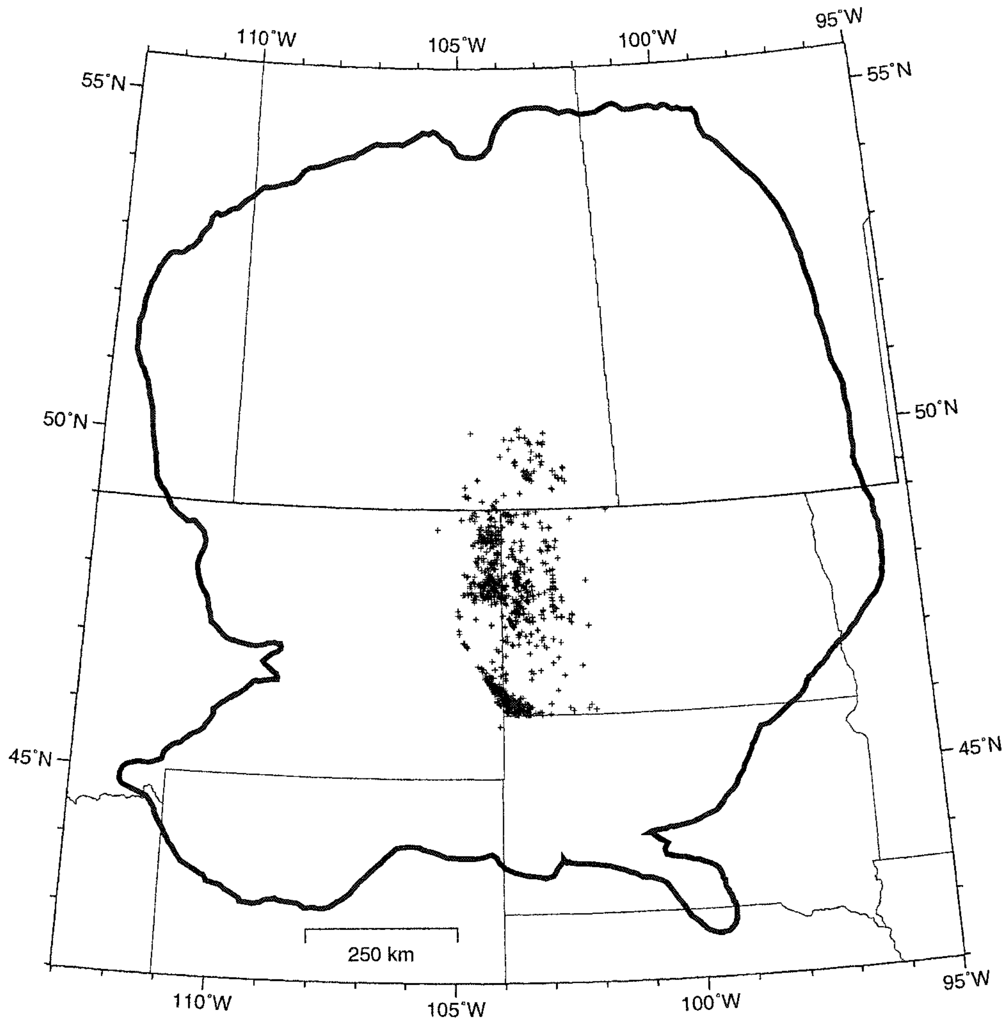

Figure 4.5 Locations of production wells. Data current to the end of August, 2000. South Dakota data were not reported due to incomplete location coordinates.

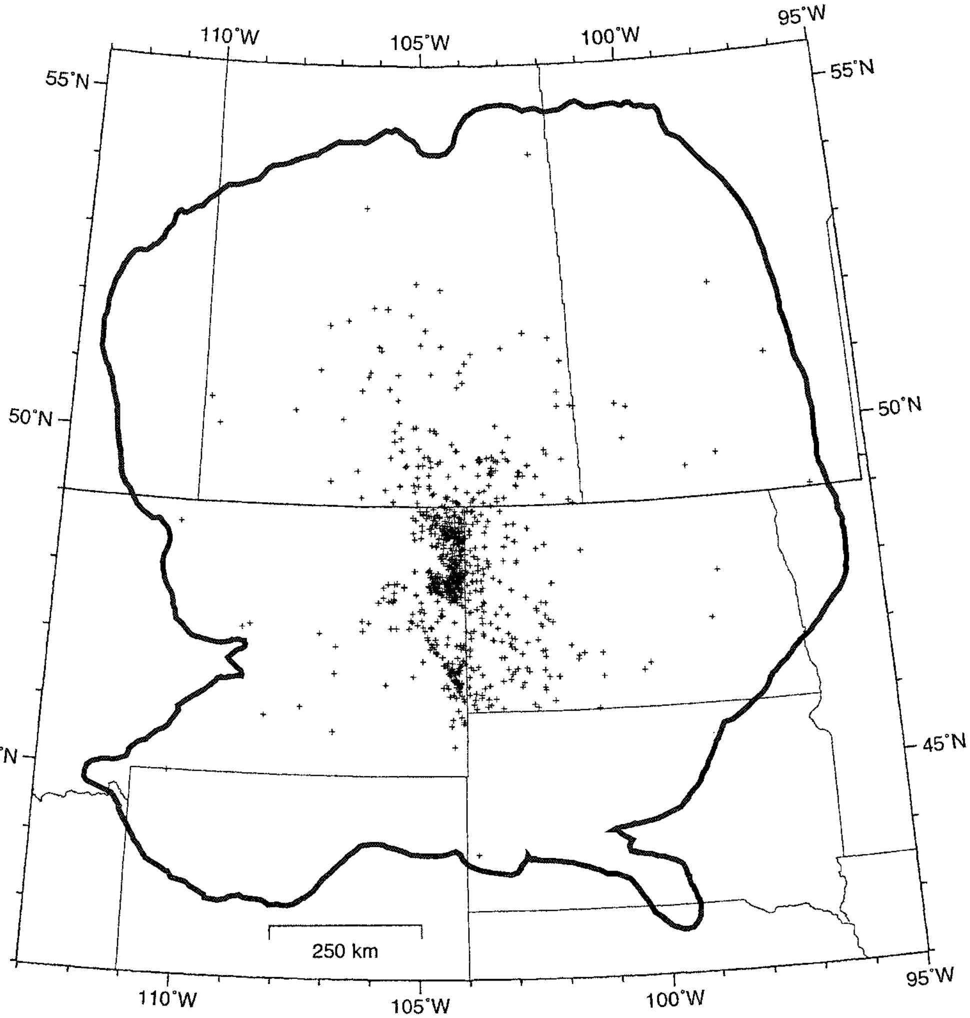

Figure 4.6 Locations of unculled pressure datapoints

Chapter 5 – Results and Interpretation

Using the previously mentioned sources and processing techniques, the hydrogeology and geochemistry of the Red River Formation in the Williston Basin, Canada-USA, was investigated. Due to the regional scope of the study, local features and phenomena were not studied in detail.

5.1 Structure

The study area occupies a gently sloping region (Figure 2.1) within the Western Canada Sedimentary Basin. Rocks of the Red River Formation are exposed at the southern, southwestern edge of the basin, as well as along the northeastern edge in Manitoba and Saskatchewan (Figure 1.1).

Isopach and structure contour maps on top of the formation for smaller, restricted areas (oil and gas fields, diminutive study areas, provinces, states) have been previously generated (e.g., Kreis and Haidl, 1997 for Saskatchewan; Bezys and Conley, 1998 for Manitoba; Gries, 1981; Brown et al., 1984 for the U.S. part of the basin), but large-scale ones, across the international border, have never before been available.

The Red River Formation and the entire basin reach their deepest points in western North Dakota, close to the Montana state border (Figure 4.1), where the thickness of the formation exceeds 210 m (Figure 4.2). The chaotic thin and thick areas indicated on the United States Geological Survey map in southern Montana and northern Wyoming have not been drawn on Figure 4.2 due to lack of control points. Both maps show that during Ordovician time, the Williston Basin became a major centre of deposition. The Red River Formation thins to the edges of the basin to various degrees: more steeply towards northeast and southeast then to northwest or southwest. A smaller-scale isopach map (Kreis and Kent, 2000) shows thinning over some of the Precambrian basement paleotopographic highs in southeastern Saskatchewan. Also, structural highs on the Precambrian surface coincide with structural highs on the top of the Red River (ibid.). These areas represent higher hydrocarbon production.

5.2 Water Chemistry

Chemical signals such as solute ratios, concentrations, changes in hydrochemical facies may indicate important geochemical processes. Regional trends can be demonstrated by using concentration maps, trilinear diagrams, ionic ratio plots, or graphs that indicate consistent patterns.

Figure 5.1 is a map of total dissolved solids (TDS) in the Red River Formation. Maximum total ion concentration (over 400 g/l) occurs near the center of the basin. The high-density brine area indicated by others (e.g., Downey, 1984) is surrounded by the 200 g/l contour line, and roughly coincides with the extent of the Lake Alma Anhydrite, which is the most widespread Lower Paleozoic evaporate unit. The 300 g/l contour coincides with the extent of the Coronach Anhydrite. The boundaries of the two anhydrite units in Saskatchewan are shown by Kreis and Haidl (1997). The highly saline waters in this part of the formation are believed to be part of a sluggish/stagnant flow system, relative to elsewhere in the basin. Therefore, because this zone is impeding fluid flow (either having it deflected around the brine or hindering it), there is an increase in residence time. The increased time allows for more dissolution (Tóth, 1984), thus higher TDS values are measured in and near this zone.

The lowest salinities occur at exposed areas where concentrations below 10 g/l are measured, reflecting meteoric recharge and/or mixing (Benn and Rostron, 1998). Generally, TDS decreases with increasing distance from the deepest segment of the formation, and decreases with decreasing depth. The two exceptions are the northwestern flank (higher than expected) where the Williston Basin joins the Alberta Basin, and the southern Saskatchewan-northern Montana area, where a large freshwater tongue is located (Benn and Rostron, 1998). An obvious reason for having low salinities along the northern and eastern flanks of the Red River is dilution due to mixing with freshwater at shallow depths.

It is worth noting that producing Red River fields are associated with high TDS concentrations: a large percentage of the producing wells (Figure 4.5) lie within a region of salinities greater than 300 g/l (Figure 5.1). Noticeable oddities are the South Dakota production areas (e.g., Lantry Field); however, fairly sparse control may be blamed for this.

Correlation between water density and TDS was examined (Figure 5.2). Very good linear correlation ($R^2 = 0.9779$) was obtained. The plot helped recognize misreported density or concentration values.

Representation of chemical data can be achieved by illustrating the major ion composition. Graphic plots allow for rapid identification and classification of water types. Piper's trilinear plot (1944) lets certain cations and anions of several samples to be drawn on one single graph in which groupings are inspected visually. Based on the diagram (Figure 5.3), where the concentration units are in milliequivalents per litre, three types of water are present in the formation, in agreement with previous work (e.g., Benn and Rostron, 1998).

The dominant ion facies in the Red River Formation are chloride and sodium, with moderately high calcium content. The samples with high (>70% meq/l) and somewhat high (20-40%) sulfate lie in the area of the freshwater tongue, and in the northern part of the study area in Saskatchewan. They are characterized by low (<20 g/l) TDS. At the same locations, the carbonate and bicarbonate proportions are elevated, while the chloride and sodium-potassium are relatively low. The calcium is high here, as pointed out by Benn and Rostron (1998). This composition forms the first distinctive type of water ($CaSO_4$) in the Red River Formation of the Williston Basin, typical of waters from the active segment of the flow system.

Waters with moderately high to high TDS (50 to 300 g/l) develop the second large group. Chloride-ion becomes dominant (at a concentration of as low as 100,000 mg/l), representing at least 80% of the anions. Calcium markedly loses relative importance, while sodium-potassium becomes the most influential cation. Benn and Rostron (1998) claim that SO_4 is higher for this type than in the $CaSO_4$ water type. However, this study found that sulfate is significantly lower (<20%) than in the previous water type. This composition suggests a less rapid hydrodynamic flow (Collins, 1975).

In the central segment of the basin, where the depth of the Red River Formation is more than 2000-2500 m deep, waters with very high TDS occur (>300 g/l). They consist almost entirely of chloride for the anions; sulfate content is very low. Calcium becomes as abundant as sodium-potassium, while magnesium is very low throughout the formation (<20% of anions). These characteristics represent the third group, the sodium-calcium chloride type waters, indicating a system of little hydrodynamic movement.

The previously depicted TDS and ion distribution fits the anion-evolution sequence observed by Chebotarev (1955). However, owing to a lack of abundant samples from elevated areas, recharge patterns could not be evaluated.

Contour maps of selected ions are shown in Figures 5.4 and 5.5. Water in the Red River Formation generally has concentrations of dissolved solids in excess of 10 g/l; near the depocentre of the basin values as high as 400 g/l are reached. Most of the increase in TDS comes from increases in concentrations of chloride and sodium. The highest concentrations of dominant ions are measured in the middle of the basin, in northwestern North Dakota, coinciding with the deep part of the Williston Basin, or in southeastern Saskatchewan. Towards the edges, values of chloride and the cations diminish gradually. The dominance of chloride and sodium, compared to other ions, is clearly indicated in Figures 5.4a and 5.5c.

It was suggested by Jankowski and Jacobson (1989), and Paul (1994) that ratios of Mg^{2+}/Ca^{2+} and SO_4^{2-}/HCO_3^- increase, while HCO_3^-/Cl^- and SO_4^{2-}/Cl^- decrease, with increasing salinity and in the direction of groundwater flow. None of these relationships proved to be entirely true for the Red River (not shown); however, certain trends are evident. The ratios of Mg^{2+}/Ca^{2+}, and HCO_3^-/Cl^-, SO_4^{2-}/Cl^- are higher close to exposed areas and remain consistently less than 2 and 1, respectively. Rocks in uplifted areas lack dolomite (Downey, 1984); therefore calcium dominates in recharge waters. At the end of the flow paths, in Manitoba, calcium is possibly removed by precipitation and the magnesium to calcium ratio increases. Ratios of bicarbonate to chloride and sulfate to chloride show an inversely related trend to the concentration of dissolved solids: in samples with TDS of less than about 100,000 mg/l, they are greater than 0.5. Throughout most of the study area, the ratio of sulfate to bicarbonate is greater than 1, and values up to 35 occur on the flanks; however, recharge waters cannot be characterized with great certainty.

The relationship of TDS to individual ions was examined (Figure 5.6, Type I, II, and III waters are circled with red, green, and brown, respectively). In general, concentrations of chloride and sodium increase consistently with increased salinity. The linear relationship was anticipated since both are dominant in the 100,000 to 400,000 mg/l, and 100,000 to 300,000 mg/l TDS interval, respectively. At about 350,000 mg/l TDS, the concentration of sodium-ion starts to decrease, as NaCl reaches its solubility. At low TDS (<10,000 mg/l) the chloride distribution is scattered since at the beginning of the flow paths groundwater has not evolved into a phase where it becomes dominant.

Water in recharge areas usually shows an elevated level of bicarbonate-ion content, consistent with Chebotarev's sequence (1955). However, in the Red River Formation bicarbonate remains at low concentrations throughout. This could be the result of exchange with sulfate-ion, or poor analysis.

Because anhydrite is generally present over the study area, its dissolution will result in a quick evolution to the sulfate-phase. At higher TDS, the release of calcium-ion in the process of dolomitization may cause precipitation of sulfate minerals, thus reducing sulfate concentrations (Busby et al., 1995).

There is a larger scatter for calcium and magnesium, but the increasing trend can easily be traced. Deep in the basin, both ions are characterized by high concentrations

(Figures 5.5a and 5.5b). Both calcium and magnesium ion concentrations increase with increasing salinity. It is well known that dolomitization ($2CaCO_3 + Mg^{2+} = CaMg(CO_3)_2 + Ca^{2+}$) was an important process in the Red River Formation (e.g., Martiniuk et al., 1998). Both calcite and dolomite occur in the system; therefore, they may dissolve simultaneously. If groundwater dissolves dolomite first, then moves into an area where calcite dominates, the water will dissolve calcite, causing the water to become supersaturated with respect to dolomite (Freeze And Cherry, 1979).

5.3 Temperature

Flow of groundwater can play an important role in the distribution of heat patterns in sedimentary basins. Depending on the flow velocities, the geothermal regime may be distorted. Despite the fact that temperature influences transport processes, the present study does not focus on a full and exhaustive characterization of heat flow, mainly due to a lack of data in the Canadian portion of the basin (Figure 4.3). This section is included in this thesis to serve as an additional tool to define the flow system, or to determine whether or not there is a link between flow and heat. It has been shown at other locations (e.g., Alberta Basin by Hitchon, 1984) that moving groundwater plays a crucial role in the development of geothermal patterns, therefore it is expected that temperature variations in the Williston Basin may reflect the effects of flow.

Temperatures of water in the Red River Formation range from 20 to 171 ^{0}C (Figure 4.3). Lowest values occur in recharge areas in southern Montana and western South Dakota, and in discharge zones in eastern North Dakota, Manitoba, and along the northern edge of the study area in Saskatchewan. Highest temperatures occur in the deepest part of the basin. The shape of the contour lines resembles that of the structure map; the pattern is not by chance. The thick sequences of Mesozoic shales are poor conductors of heat (Gretener, 1981); hence, these rocks can form an insulating blanket, which retains heat from the basement. The average geothermal gradient, defined as the ratio of the temperature difference between the surface (a fixed temperature of 5 ^{0}C according to Judge (1973) and Jones (1991)) and the bottom of the hole to the depth of measurement, agrees with what is regarded "normal" (25-35 ^{0}C/km) in sedimentary basins (Gretener, 1981). The presumed active groundwater flow in the shallower parts of the basin (Downey, 1984) should transport heat away from rocks causing lower temperatures and lower average thermal gradients. Whereas, in the high-density brine area the minimal water circulation conditions should enhance heat retention. Moreover, crude oils that occur within or close to the brine zone, have low thermal conductivity, and are good insulators. This property, supplemented by the influence of the sluggish brine (which tends not to transport heat), should result in an increase of the average geothermal gradient towards the shallow part of the basin. Unfortunately, the map of the geothermal gradient (not shown) is inconclusive. Furthermore, due to poor data resolution in the USA, temperature distribution seems to not contribute to a better understanding of the system.

Bachu and Hitchon (1996) claims that the absence of thermal anomalies indicates weak groundwater flow in the Williston Basin, which prevents the induction of advective disturbances of the geothermal regime. This is supported by the proposal by Deming and Nunn (1991) who argued that if advective effects were strong enough to disturb the thermal regime, all brines would be flushed out from the basin. In the Williston Basin this cannot be the case, because the brine is just partially flushed out. On the other hand, reported elevated temperatures at oil fields permit the assumption that convective heat transport might be an important factor in certain parts of the basin. The question will surely be a subject of extensive research in ensuing years.

5.4 Oil Density

As hydrocarbons migrate along a porous carrier bed, their composition will change continuously (Silverman, 1965). Their distribution may elucidate migration patterns, but oil density variations can be subtle and extremely difficult to interpret. If oil and gas are present along a pathway as separate phases, the lighter components should occupy the first structural traps due to buoyancy effects (Gussow, 1954). As a consequence, oil will fill the farther traps, resulting in an increase in oil density in the direction of the flow. For stratigraphic traps the reverse trend prevails, as the lighter components will leak out due to enhanced buoyancy pressures. More complex differentiation patterns can be developed due to other factors such as the existence of combination traps, depth, timing of generation and expulsion from source rocks; however, these will not be considered here.

Oil pool densities show a great variation in the Red River Formation from 620 to 760 kg/m^3. In Bowman County, North Dakota alone it varies between 680 and 750 kg/m^3. A larger scale map (not shown) implies an east-, northeastward increasing trend. This would favour a separate phase migration with structural differential entrapment (Schowalter, 1979). It is well documented (e.g., Kerr, 1988) that structure plays an important role in entrapment in the Red River Formation. Many of the pools in the U.S. are located on large structures such as the Cedar Creek Anticline. Some pools in Saskatchewan (Minton, Lake Alma, Hummingbird) are connected to basement related closures (Martiniuk et al., 1998). On the other hand, stratigraphic traps due to dolomitization and porosity development may exert the opposite relationship between density and migration direction. Although it can vary locally, the general trend seems to be increasing oil density towards east, northeast.

5.5 Pressure and Fluid Potential

In a sedimentary basin with sloping flanks, regional groundwater flow patterns develop, where water flow is descending, lateral, and ascending at recharge, midline, and discharge zones, respectively. Its velocity, depth, and extent are all dependent on the position in the basin. Furthermore, topographic changes result in the occurrence of different types of flow systems. The measured formation pressures, pressure differences obtained by comparison to nominal hydrostatic values, and other derived applications (e.g., UVZ-maps, shown later) help characterize flow, thereby improving exploration efficiency. The most important parameter for the flow to be represented is the fluid potential of formation fluids.

A pressure-depth plot was made for the Red River Formation using culled DST pressure measurements. All of the data plot below the hydrostatic gradient (Figure 5.13), indicating that the centre of the basin is underpressured. It also shows that water pressure data have a similar gradient with respect to the hydrostatic rate of pressure change.

5.5.1 Interference Index

After obtaining of the acceptable quality DST's, as described in section 4.1.6, further manipulation of the dataset was necessary to eliminate pressures disturbed by earlier production (section 4.1.6.1). The interference index (I) was used to further refine the group of data used for flow mapping investigation. The difficulty is deciding at what value the influence becomes significant. The number of previous studies on production induced drawdown (PID) is very limited; moreover, it has not been attempted for the Red River Formation. Thus an "introductory" value is set up, which can be a starting point for future studies in this direction.

The freshwater equivalent hydraulic head map using the unculled, production disturbed DST's (885 pressures) is shown in Figure 5.7. The region along the Montana-North Dakota border is the "noisiest" but other areas also contain incongruous tests. Interference indices range from –5.8 to 3.5. First Rostron's program had been run (section 4.1.6.1). Regardless of what radius was chosen (2 or 3 km), the contour lines did not change on the maps (not shown). It means that distance alone is not the primary factor for creating PID. The case may be that a production well locating close to a DST well might have been on production for just a brief period prior to a test. Thus, Wilkinson's modified simulation (section 4.1.6.1) was applied, taking into account the time elapsed since production started. With a series of interference numbers (I=0.6, 0.3, 0.0, -0.5, -1.0), the initial DST's 29, 34, 38, 48, 61%, respectively, were removed. I=-1.0 was recognized for threshold, at which value the dataset can be considered representative to virgin, undisturbed conditions (Figure 5.8).

5.5.2 Equivalent Freshwater Hydraulic Head vs. Buoyancy Modified Head

The use of equivalent freshwater hydraulic head assumes near horizontal aquifers, and that small density-related effects can be ignored (Hanor, 1987). For flow in variable density systems, a few authors derived a correct formulation of Darcy's Law (e.g., Bear, 1972; Garven and Freeze, 1984). Motion is caused by a force that is proportional to the negative gradient of the freshwater hydraulic head and by the buoyant force (Chapter 3).

The freshwater hydraulic heads for the Red River Formation are shown in Figure 5.8. The highest values are found in the southwestern part of the area, where ground elevations are highest. The lowest values are located in wells in the northeastern study area in Manitoba. The patterns of hydraulic head show several important features, which will be discussed in detail. The potentiometric surface has three distinctive areas in terms of distribution of fluid potentials. The southern, southwestern region is characterized by steep gradients, while hydraulic heads decrease towards northeast. These two regions surround the deep basin, which is represented by quasi-unchanged heads, with widely separated contour lines. Compared to the topography of the basin (Figure 2.1), the resemblance is salient. Steeper contour lines on one map coincide with steeper contour lines on the other, at the same location. The only exception is in the middle of the basin. In Figure 5.9, vectors show hypothetical flow directions from recharge areas towards north, then north-northeast. Greater magnitudes are indicated by longer vectors. This would be the case for isodensity flow. Figure 5.9 generally agrees with the hydraulic head distribution drawn by Bachu and Hitchon (1996) for the Basal aquifer system, and by Downey (1984) for the U.S. Cambrian-Ordovician aquifer of the Williston Basin.

However, salinities are not constant in the Williston Basin (Figure 5.1), but cover a wide range. That necessitates the incorporation of a term into the general flow equation, which represents the buoyant force, impelling a fluid particle upwards. With the method described in Chapter 3, the buoyancy modified driving force was calculated (equation 3.9). The vector diagrams in Figure 5.10, 5.11, and 5.12, show the buoyant, the buoyancy-modified, and all three (freshwater head (blue), buoyant (grey), and modified (green)) force vectors, respectively. Naturally, buoyant force vectors are missing where freshwater occupies the basin (Figures 4.4 and 5.10), and the greater the salinities the more significant the influence of buoyancy. Figure 5.10 shows that buoyant forces are significant in the middle of the basin, and weaker towards the edges, pointing to the centre part.

The investigation can be grouped into four categories. First, in central, north-central Montana, and western, central Saskatchewan, the previously dominant northward direction (Figure 5.9) did not change significantly (Figure 5.11); however, its magnitude diminished since the two forces are opposed (Figure 5.12). Second, in the central North Dakota part, the buoyancy-modified flow force is greatly decreased due to the forces that are opposite and similar in magnitude. Third, in the middle of the basin, the deviations due to buoyancy, both in magnitude and direction, are shown in Figure 5.12. Fourth, buoyancy is unimportant in Manitoba, eastern North Dakota, and southern Montana. This area is correlated with the zone of no hydrocarbon accumulations. The illustrated freshwater flow patterns are in fairly good accordance with those ones suggested by Dinwiddie and Downey (1986) for the Cambrian-Ordovician aquifer system in the United States segment of the basin.

In short, two distinctive driving forces are present in the study area: one is created by the effects of topography, while the other arises from buoyancy caused by variations in fluid density. Neglect of the effects of density would have resulted in obtaining an inaccurate flow pattern in terms of direction and magnitude at certain parts of the basin.

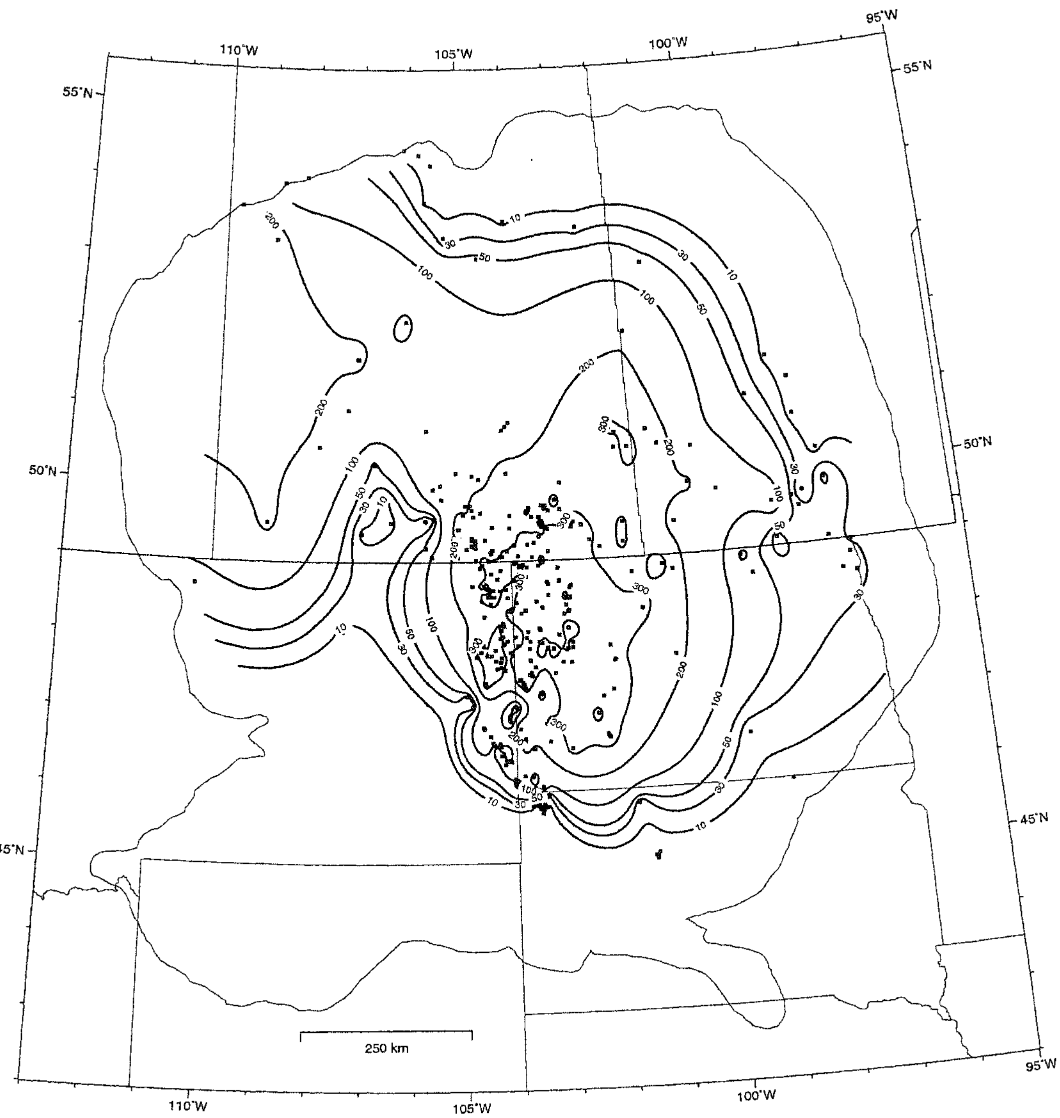

Figure 5.1 TDS of the Red River Formation (C.I. = variable, in g/l)

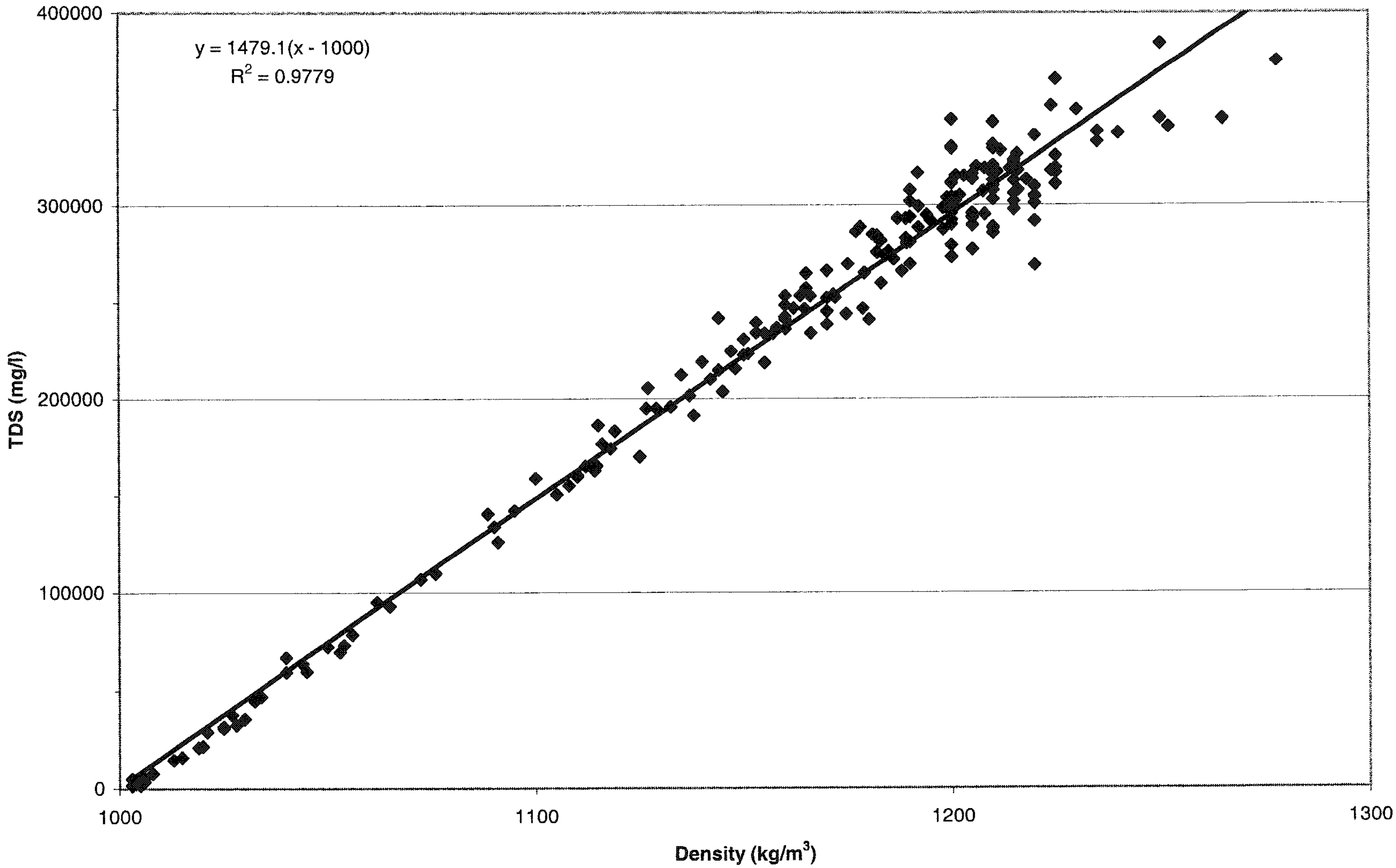

Figure 5.2 Relationship of TDS to density of formation waters

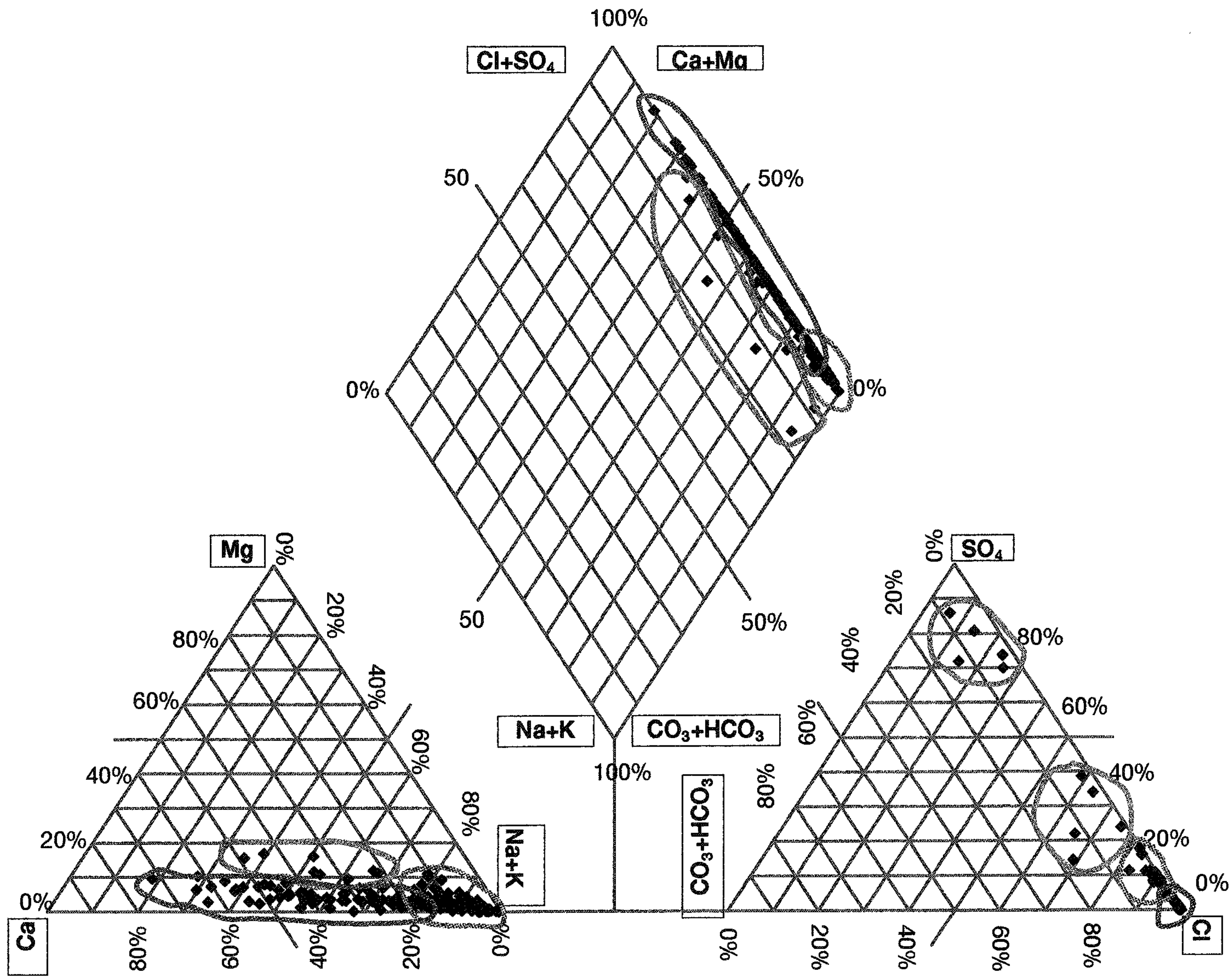

Figure 5.3 Piper diagram showing composition of formation waters in the study area. Type I waters are circled with red, Type II with green, and Type III with brown.

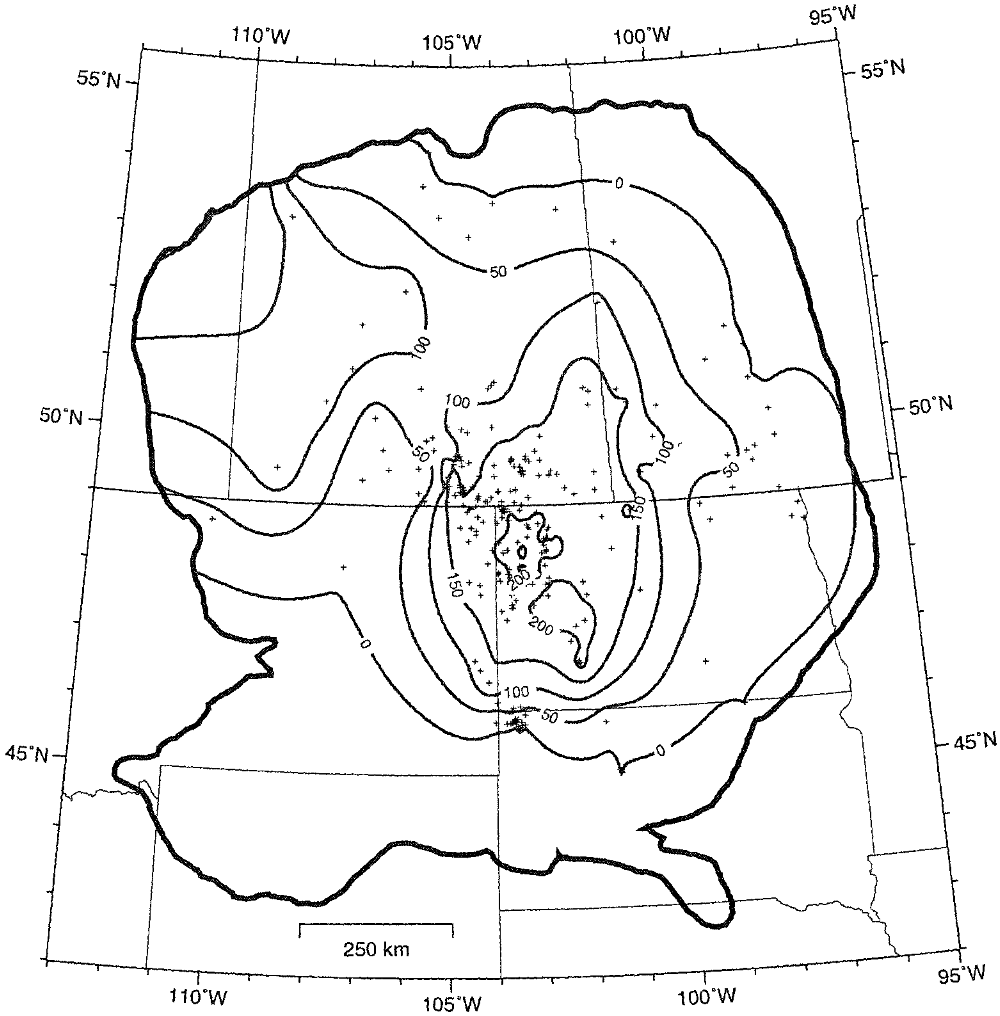

Figure 5.4a. Concentration of chloride in the Red River Formation (C.I.=50 g/l)

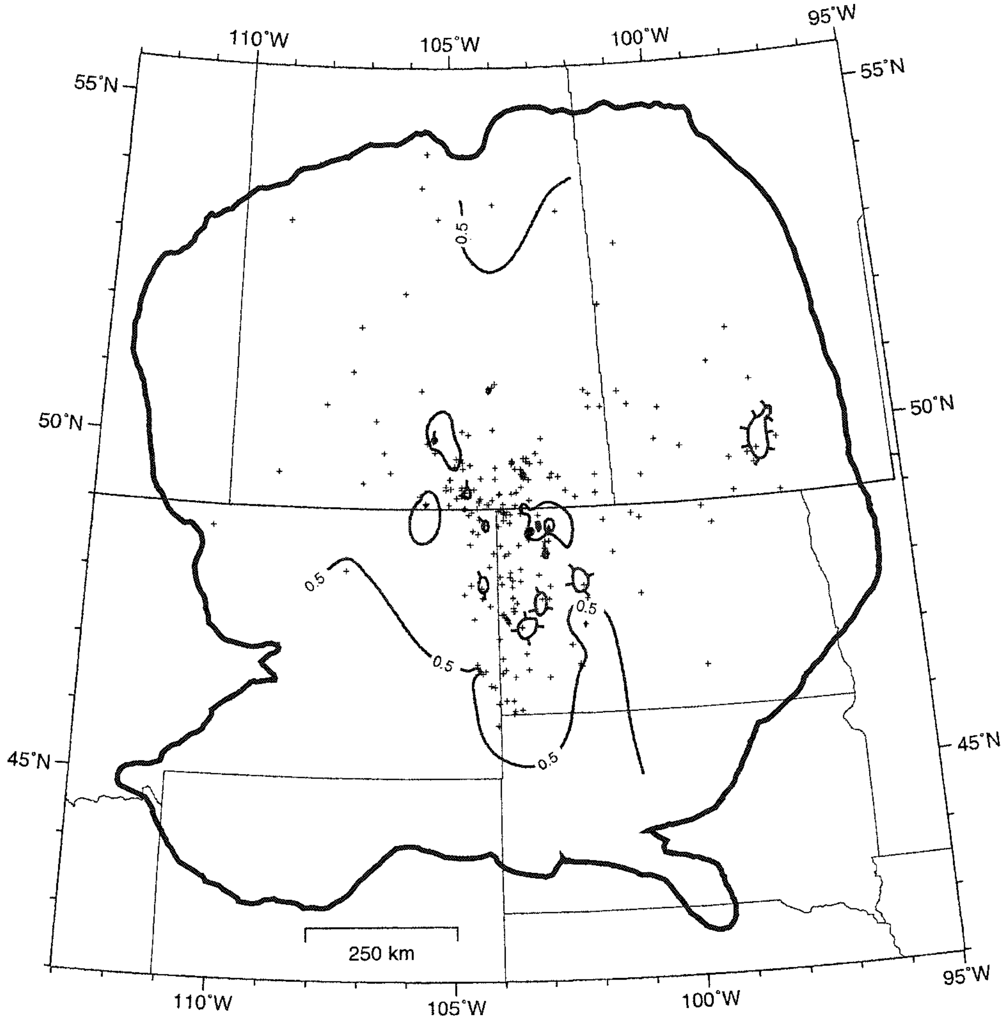

Figure 5.4b Concentration of bicarbonate in the Red River Formation (C.I.-0.5 g/l)

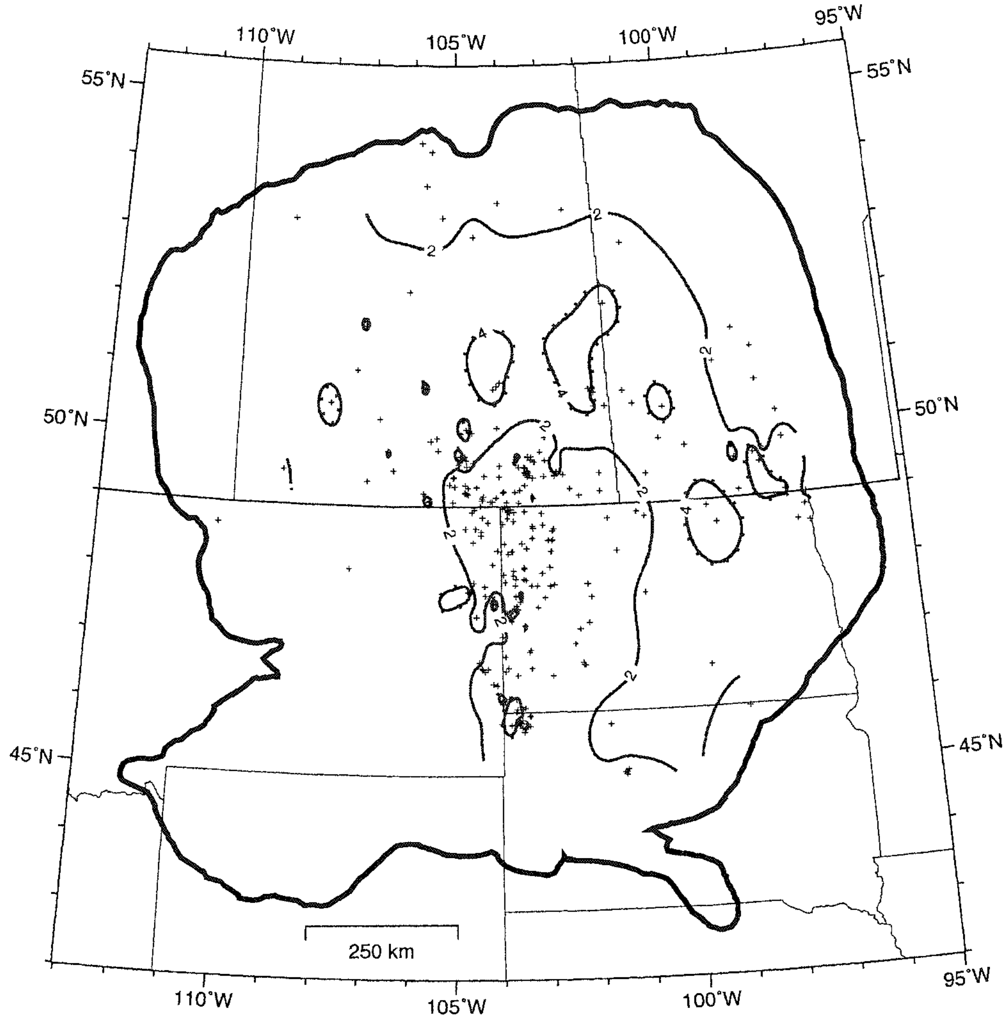

Figure 5.4c Concentration of sulfate in the Red River Formation (C.I.=2 g/l)

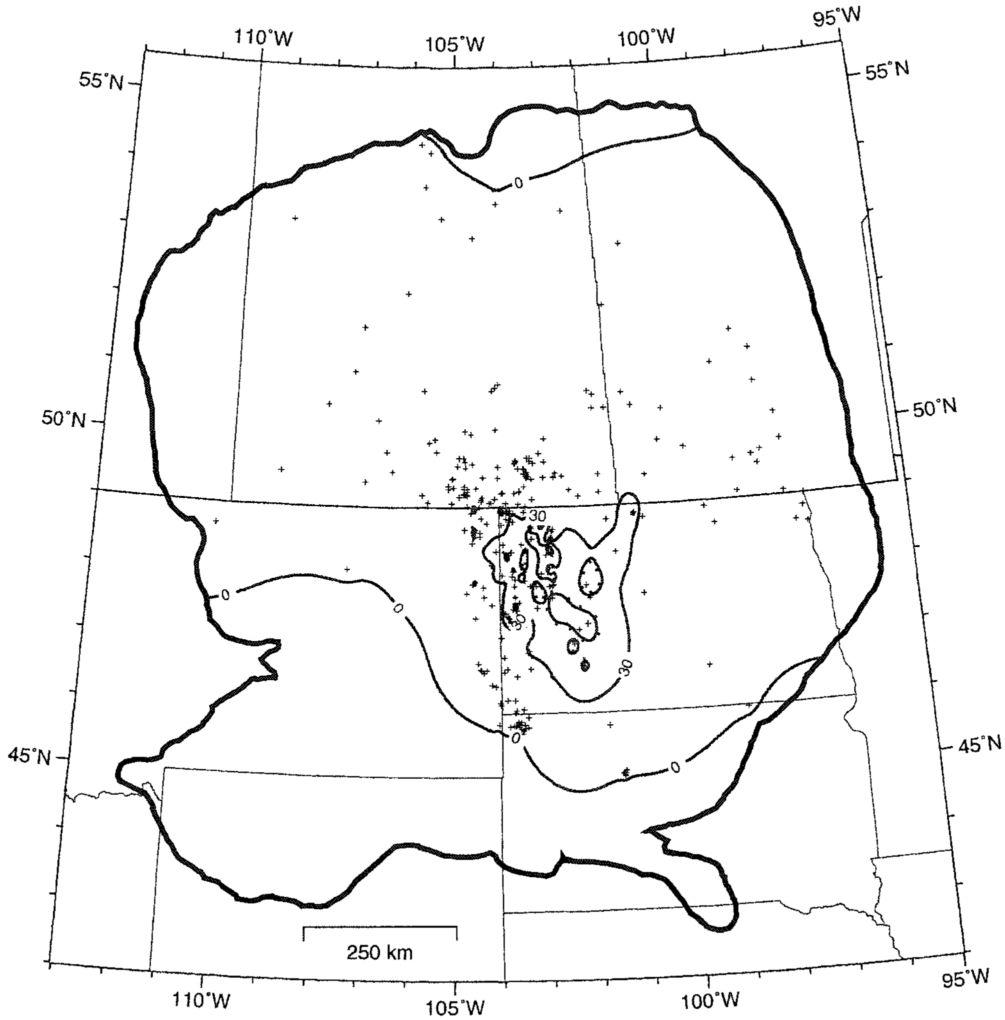

Figure 5.5a Concentration of calcium in the Red River Formation (C.I.=20 g/l)

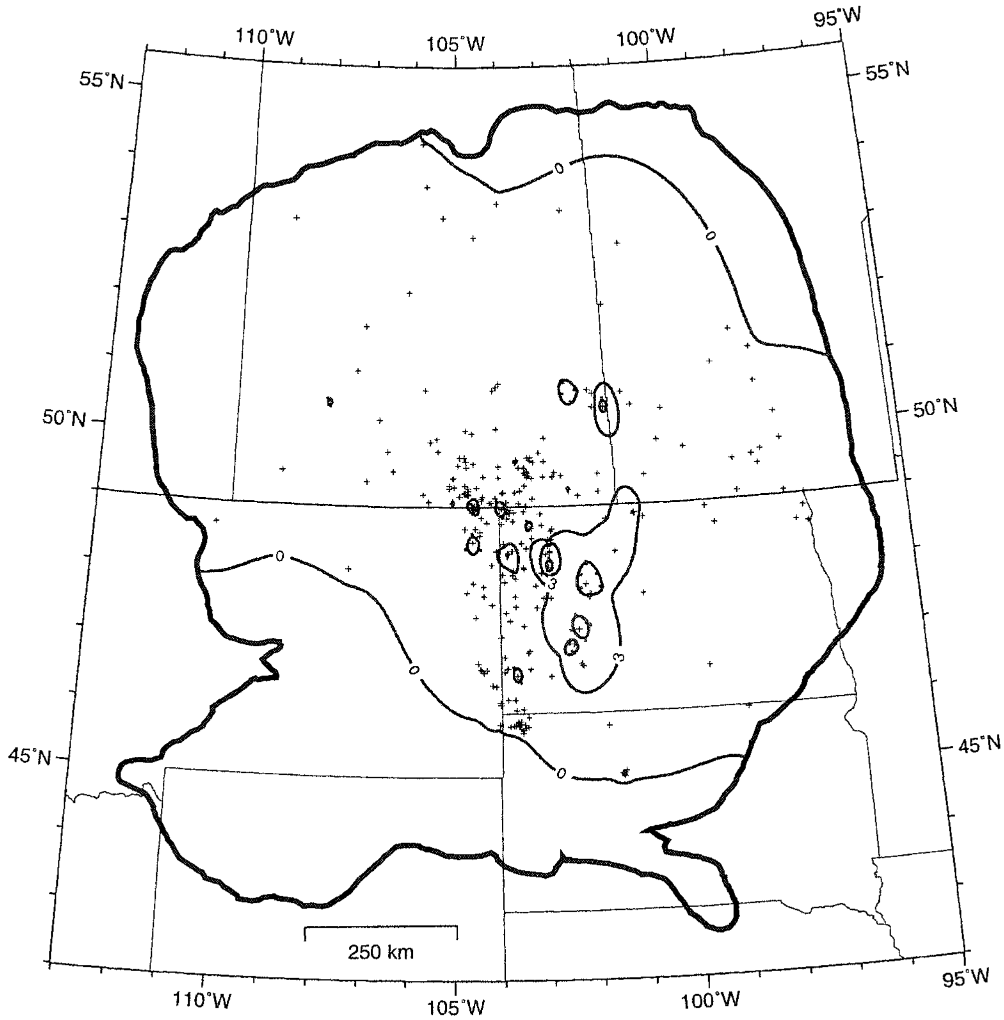

Figure 5.5b Concentration of magnesium in the Red River Formation (C.I.=3 g/l)

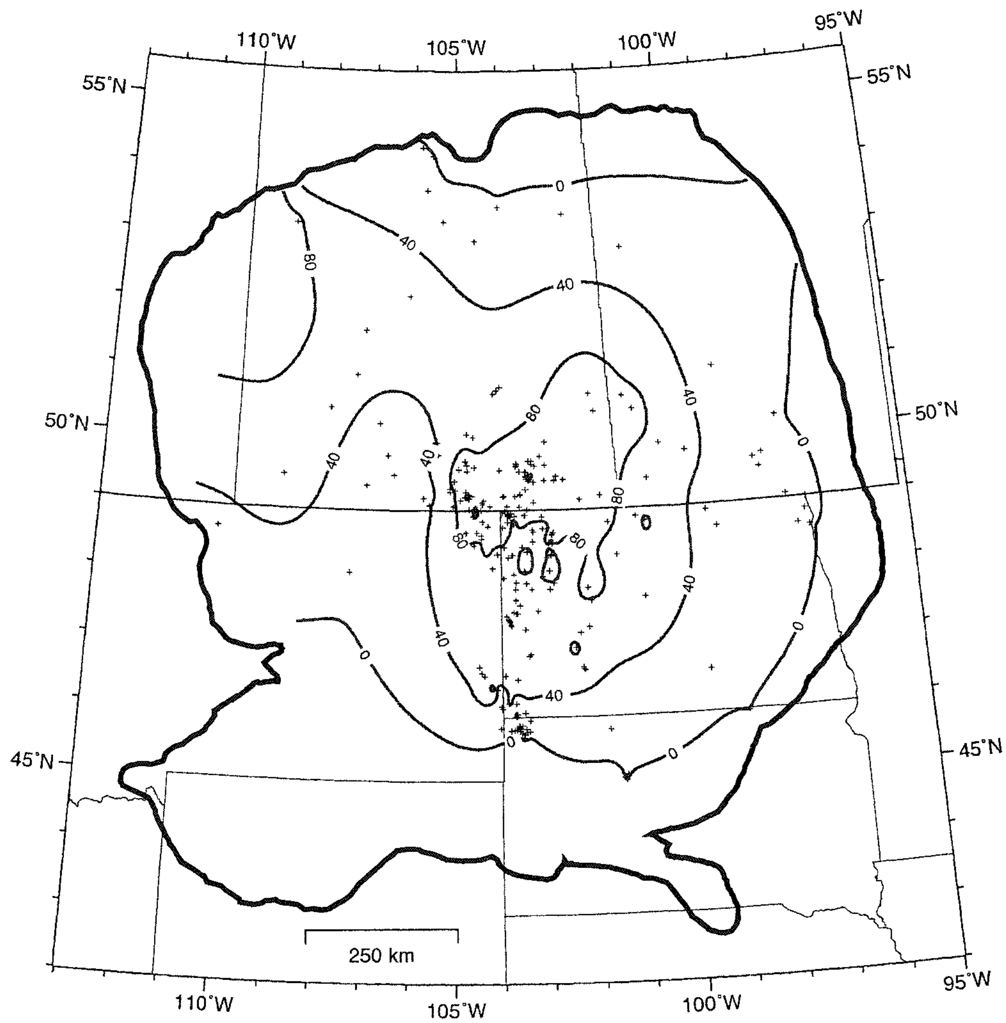

Figure 5.5c Concentration of sodium in the Red River Formation (C.I.=40 g/l)

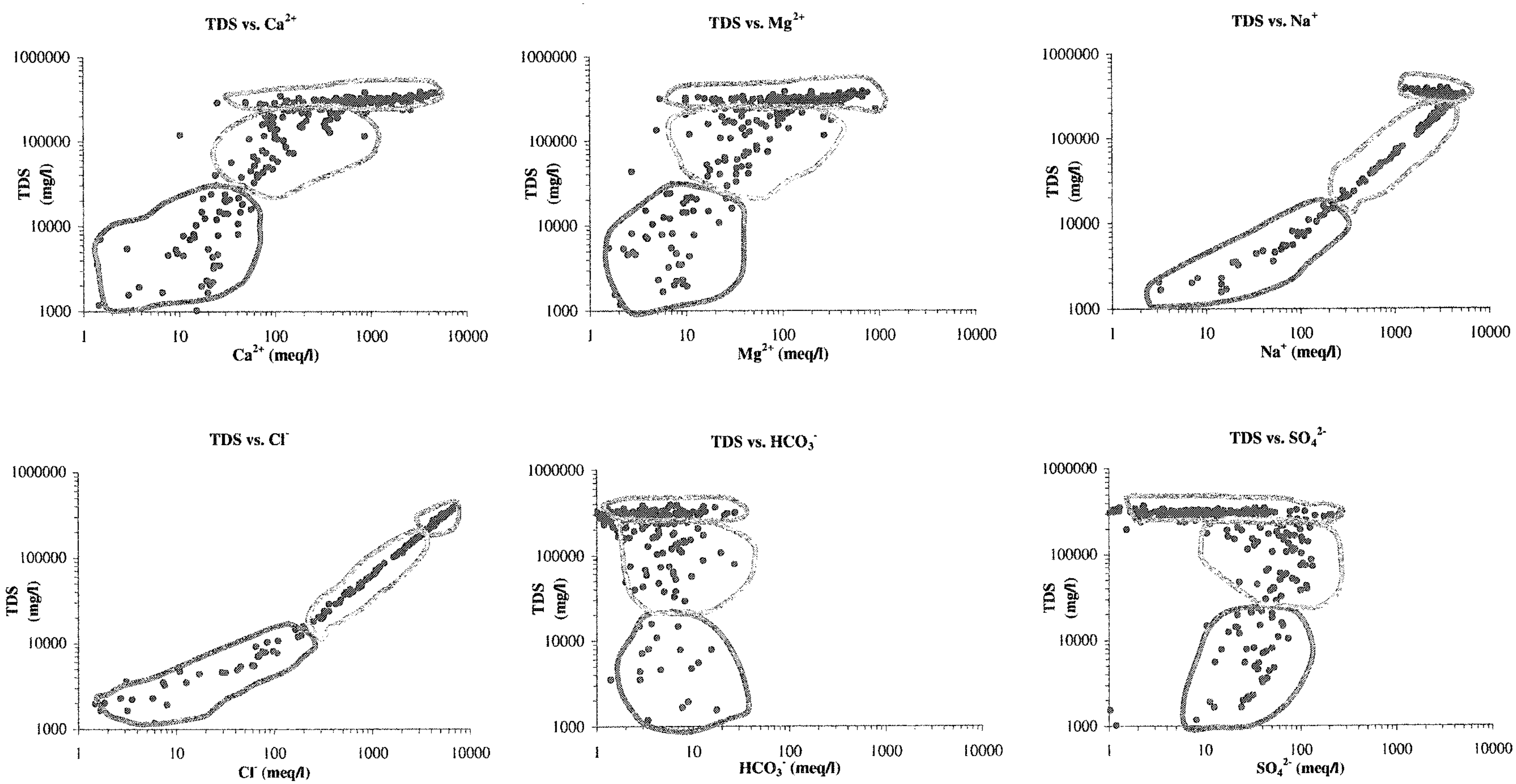

Figure 5.6 Relationship of TDS to individual ions

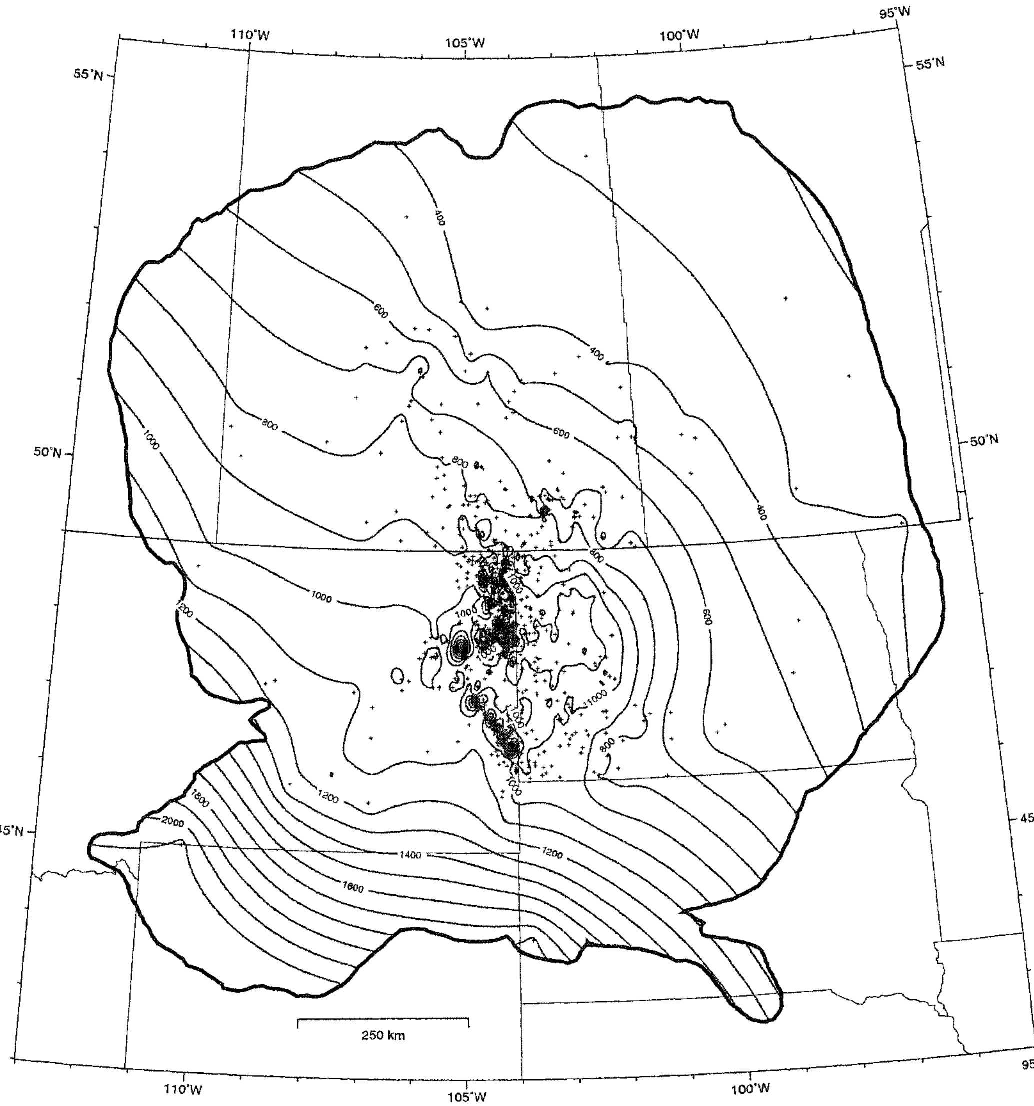

Figure 5.7 Equivalent freshwater hydraulic head contours (C.I. = 100 m) in the Red River Fm. (unculled)

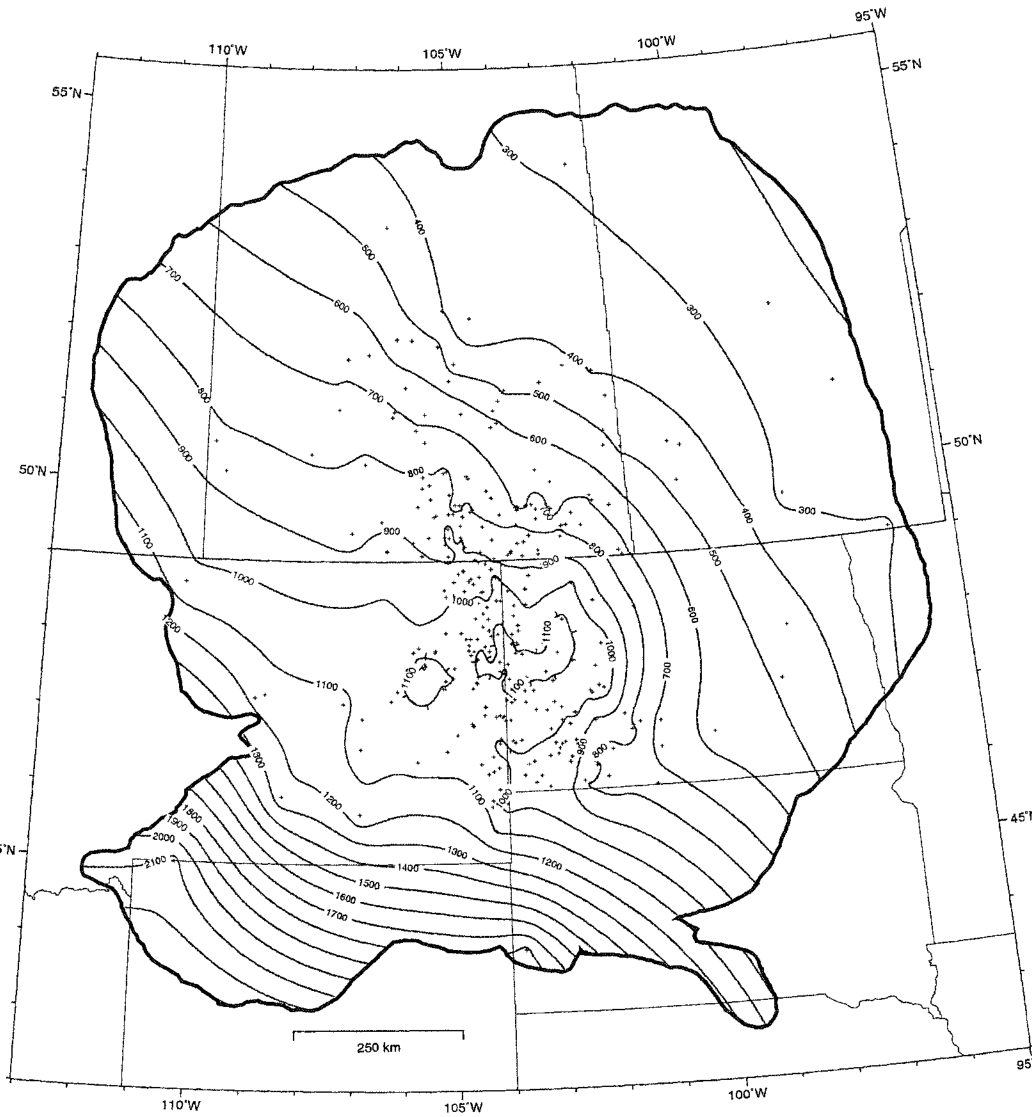

Figure 5.8 Equivalent freshwater hydraulic head contours (C.I. = 100 m) in the Red River Fm. (culled)

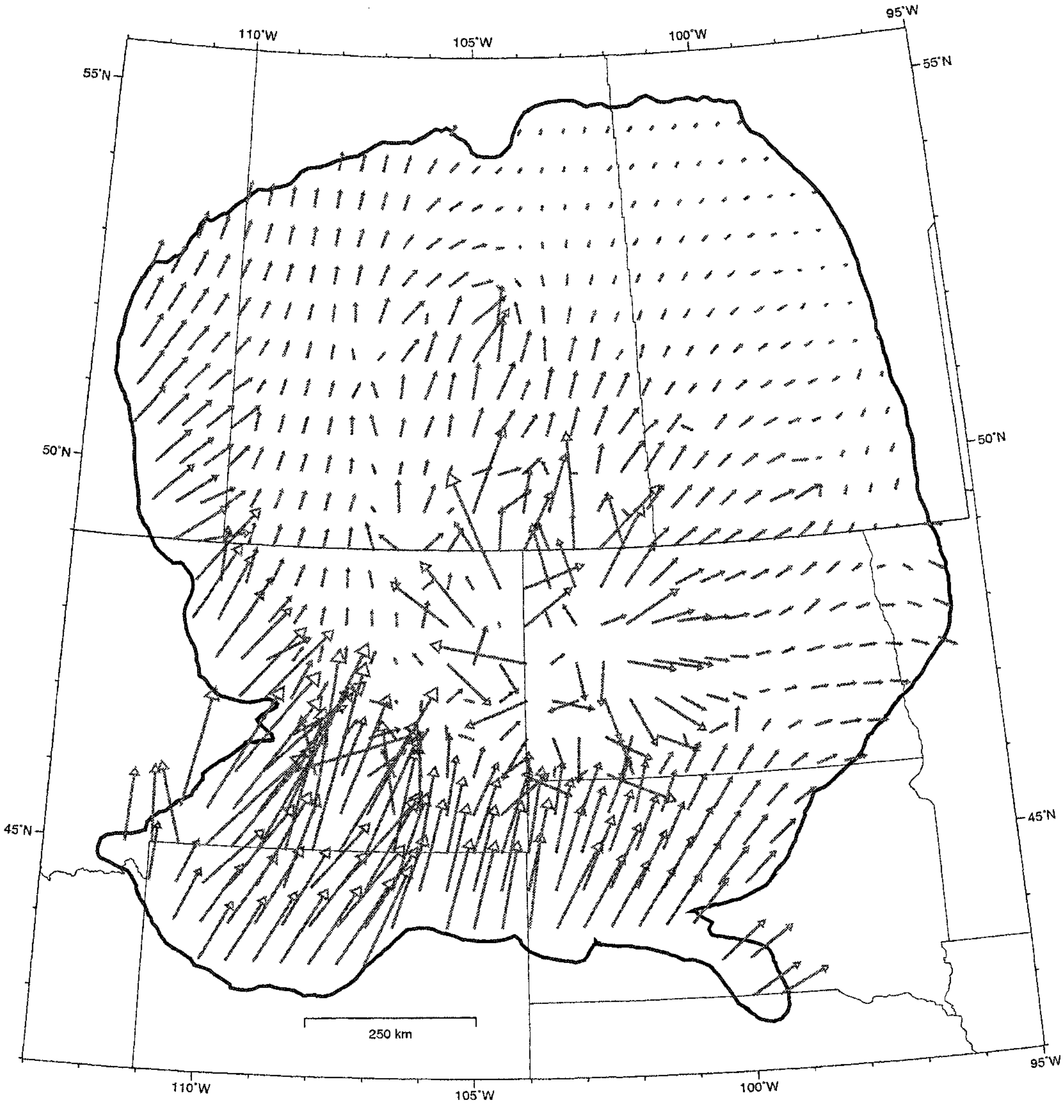

Figure 5.9 Map showing the freshwater head gradient vectors

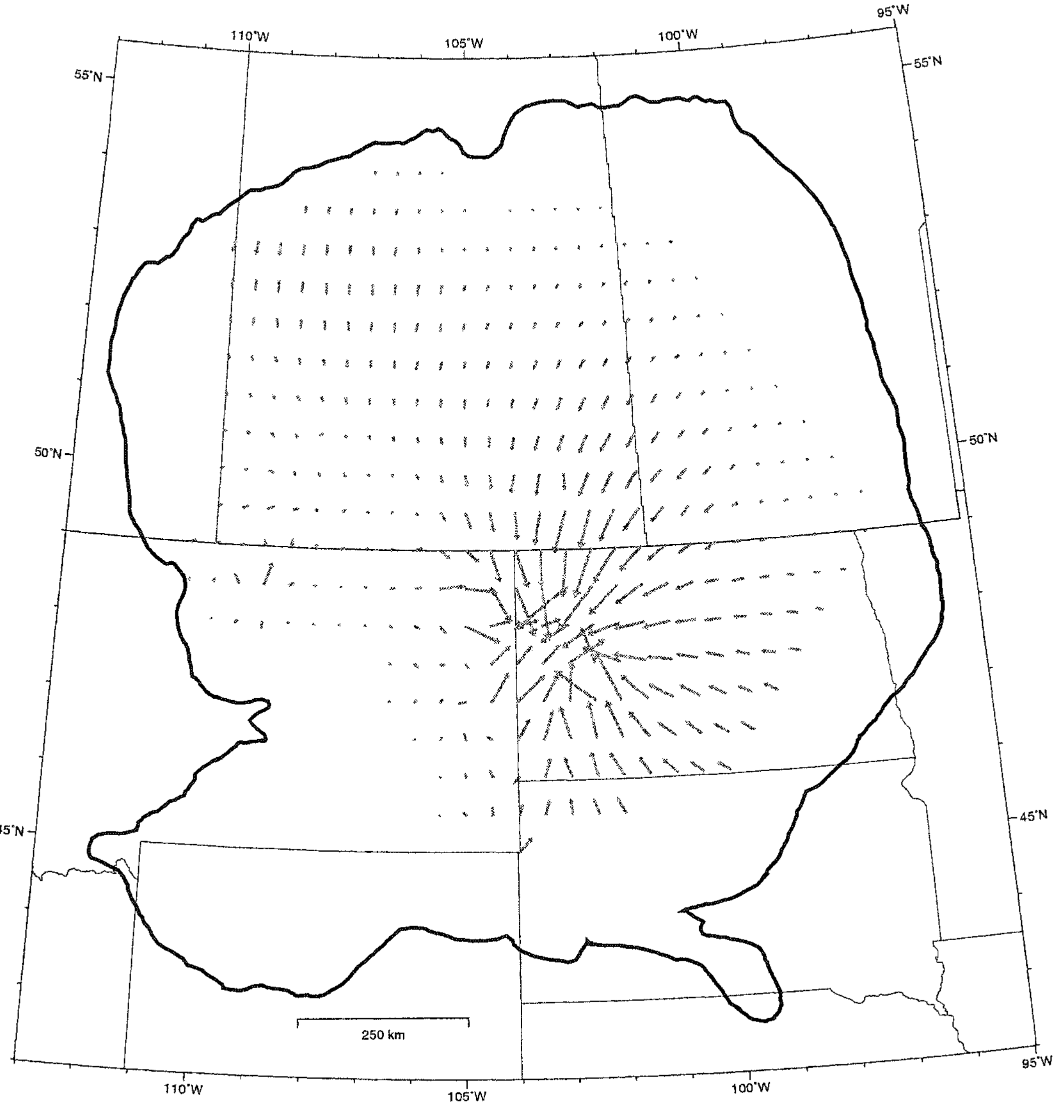

Figure 5.10 Map showing directions of the buoyant force

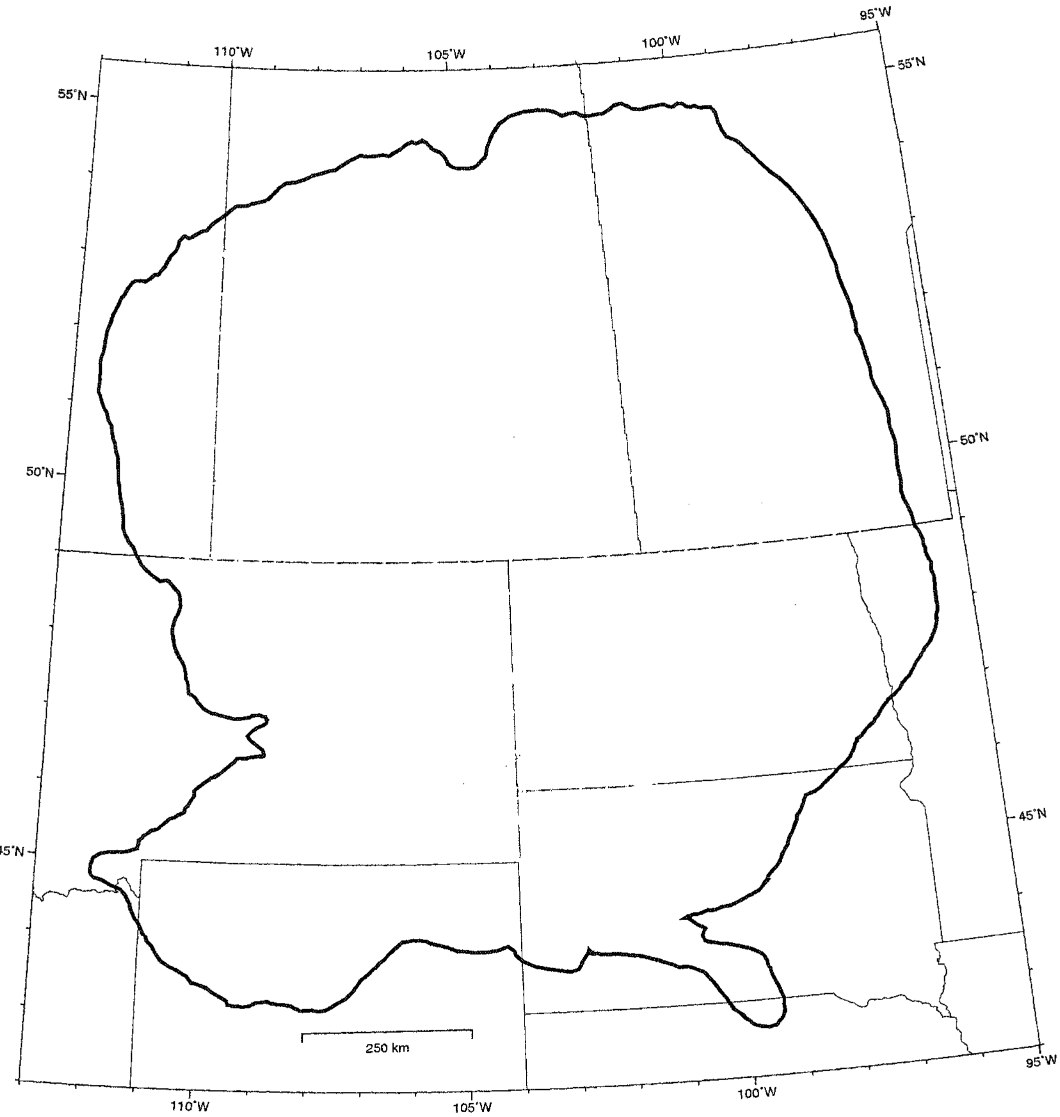

Figure 5.11 Map showing the buoyancy-modified force vectors

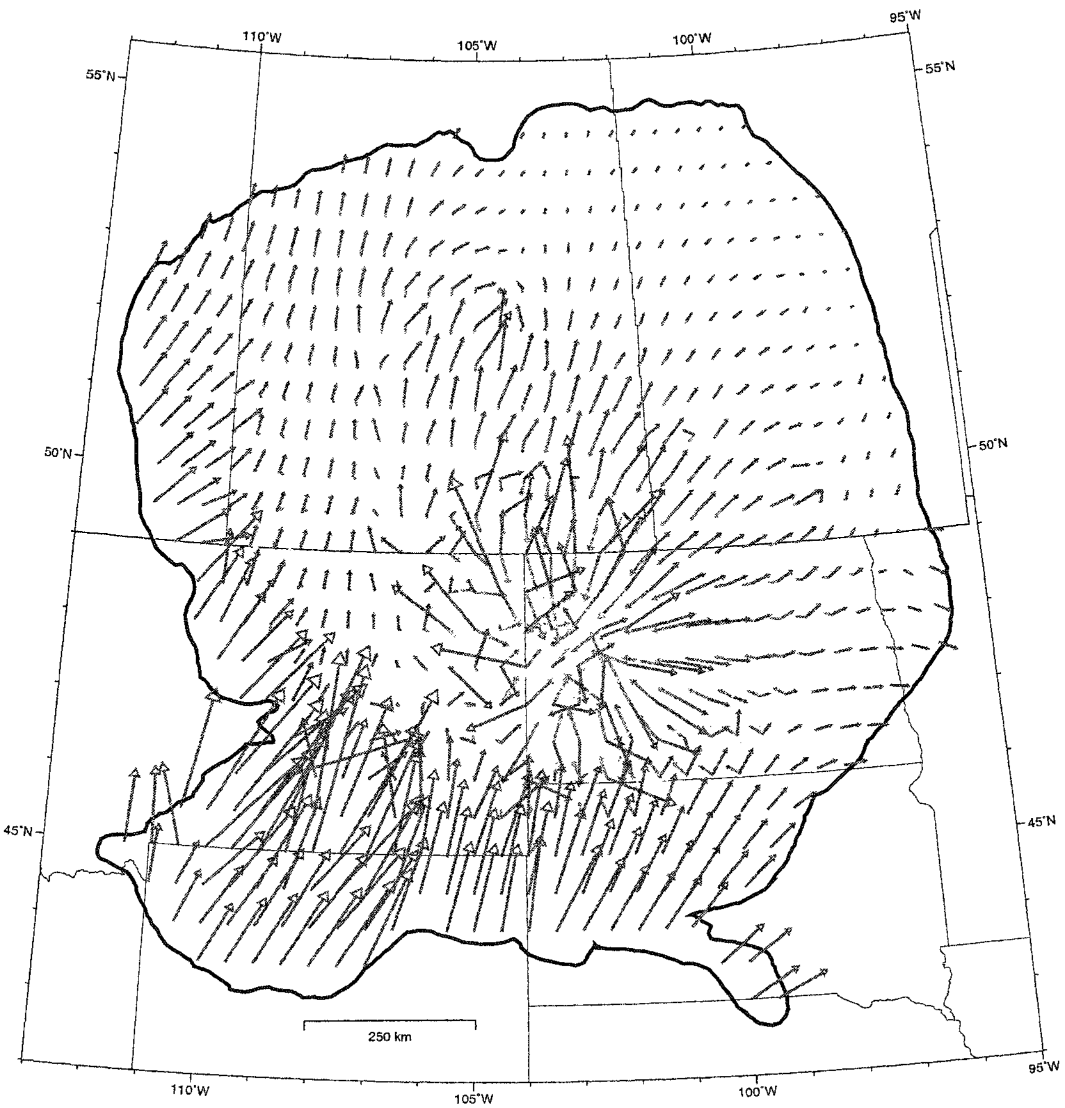

Figure 5.12 Map showing the buoyancy-modified force vectors (green), the freshwater head vectors (blue), and the buoyant force vectors (grey)

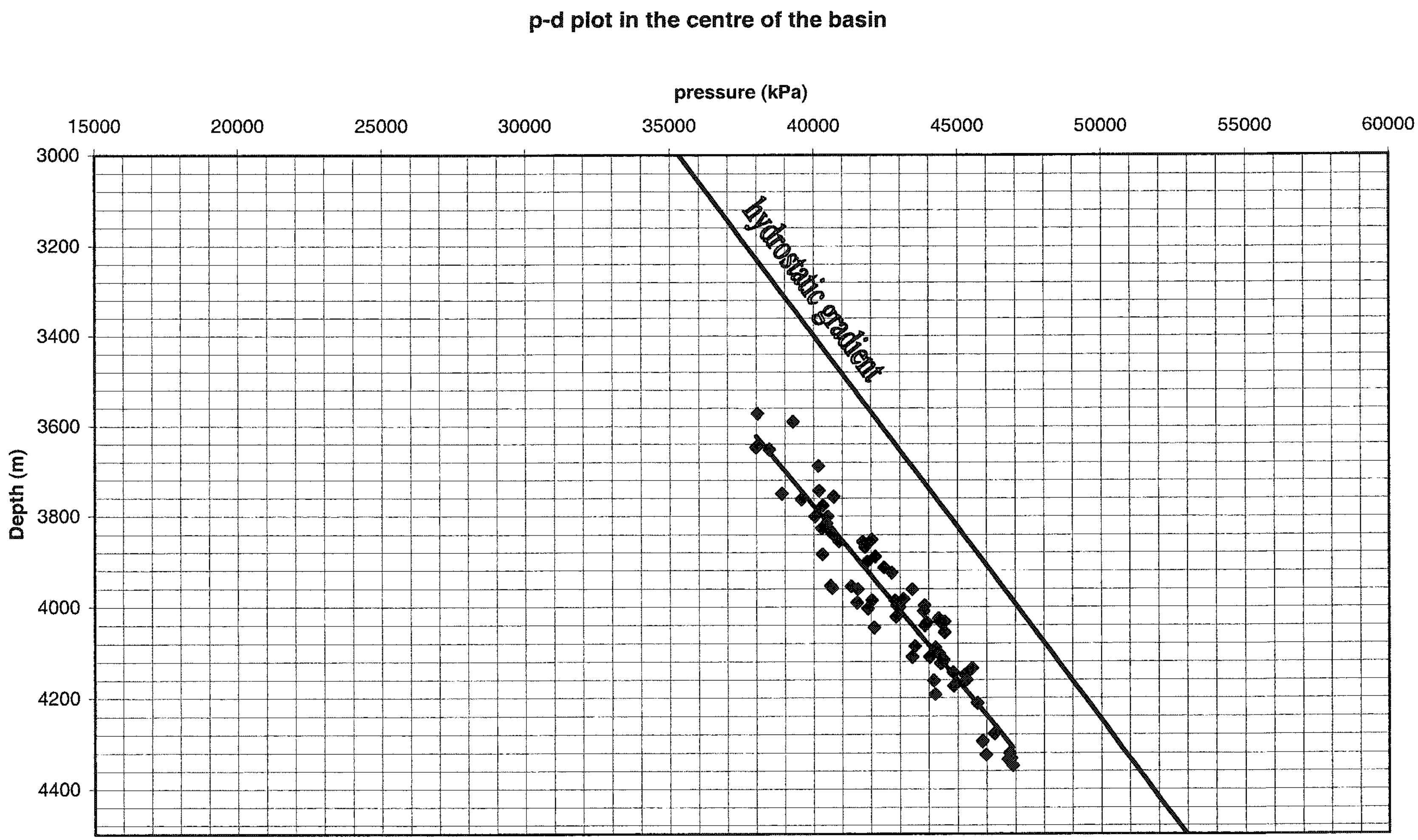

Figure 5.13 Pressure-depth plot in the centre of the Williston Basin

Chapter 6 - Application of the UVZ-method

6.1 Migration of Hydrocarbons

Movement of hydrocarbons from source rocks to reservoirs and traps occurs in three or four successive steps. First, hydrocarbons are generated and expelled from disseminated organic matter. This phase is called primary migration. Second, hydrocarbons move along a three-dimensional, dendritic network through permeable strata (secondary migration). Third, hydrocarbons are trapped due to structural, stratigraphic, diagenetic, lithostratigraphic, hydrodynamic changes. Fourth, trapped oil and gas may migrate further to another trap or to the surface as a result of a weak seal, tectonic activity, leakage, etc. (Tissot and Welte, 1978). Only the second and third steps are of interest here.

6.2 Principles of the UVZ-method

In spite of the numerous studies and research in the last decades (Martiniuk et al., 1998), the modes, forces, patterns, and mechanisms of migration and entrapment are still not completely explained. Many theories identify water as an indispensable agent that can generate and transmit forces impelling petroleum particles. Groundwater promotes the effectiveness of exploration by revealing or masking indicators related to water flow, besides transporting hydrocarbons.

In 1953, King Hubbert proposed the so-called UVZ-method, a graphical solution to indicate regions of minimum fluid potentials for oil, i.e., the potential accumulation sites. It has been applied in a few cases (e.g., Zawisza, 1986; Feng, 1997; Meissner and Banks, 2000). The mathematical background of the UVZ-method follows.

Using the equations for the fluid potential for water (equation 3.2), the oil potential (Φ_o) can be written at a given point, omitting the capillary term, as

$$\Phi_o = gz + \frac{p}{\rho_o} \tag{6.1}$$

where g is the acceleration due to gravity

z is the elevation above a datum

ρ_o is the oil density

p is the pressure of the ambient water.

By solving (3.2) for p and substituting it (because, without capillarity, the pressure at a given point in a flow system is the same for both fluids (Hubbert, 1953)) into (6.1), we obtain the oil potential in terms of the water potential (Φ):

$$\Phi_o = \frac{\rho}{\rho_o}\Phi - \frac{\rho - \rho_o}{\rho_o} gz \tag{6.2}$$

By substituting (3.4) and the corresponding potential for oil ($\Phi_o = gh_o$) into (6.2), and then simplifying to an equation where every term is expressed in units of length:

$$h_o = \frac{\rho}{\rho_o}h - \frac{\rho - \rho_o}{\rho_o} z \tag{6.3}$$

Dividing (6.3) by $(\rho - \rho_o)/\rho_o$ results in

$$\frac{\rho_o}{\rho - \rho_o} h_o = \frac{\rho}{\rho - \rho_o} h - z \tag{6.4}$$

By letting $u = \frac{\rho_o}{\rho - \rho_o} h_o$

$$v = \frac{\rho}{\rho - \rho_o} h,$$

and substituting them into (6.4), yields (Hubbert, 1953):

$$u = v - z \tag{6.5}$$

Under hydrodynamic conditions the principal requirement for hydrocarbon accumulation is the existence of fluid potential minimum for the fluid in question. In Hubbert's approach, the curves of $h = const.$ and $h_o = const.$ are the contours of the water and oil potentiometric surfaces, respectively. The contours of u and v are the functions of the hydraulic heads of oil, h_o, and water, h, respectively, modified by a ratio of fluid densities. The u and v surfaces are parallel to those of the potentiometric surfaces of oil and water. The surfaces $z = const.$ are a family of horizontal surfaces of elevation z. The contours of v can be drawn by using the water hydraulic heads (Figure 5.8) and the expected fluid densities. Then the u surface is obtained graphically by calculating and contouring the difference between v and z. The minima of the u surface will represent potential oil traps. It is a convenient solution permitting the use of the most easily available, measurable parameters, the freshwater hydraulic head and the elevation with respect to a chosen datum.

6.3 Application of the UVZ-method

6.3.1 UVZ-map of the Red River Formation

The UVZ-map in Figure 6.1 shows the same general trend in the southwestern part of the study area as the hydraulic head map for water (Figure 5.11). Calculated oil heads decrease from as high as 4000 m to less than 2500 m in eastern Montana, northeastward. There are a few minimum closures in central Montana between longitudes 107° W and 110° W, but no other latent accumulation sites are indicated at any other locations within the study area at this scale. This can be the consequence of using a too small scale; a more detailed map focusing on a much smaller region will likely reveal potential minima at the field scale. Further north- northeastward, contours are concentric and increase towards the center of the basin. If the map of areas of source rock maturity (Figure 1.1) was placed on Figure 6.1, the coincidence of the two areas (i.e., mature source rock zone and maximum of oil head contours) is observed. Since oil migrates in the 'oil potential energy' field, it is possible to indicate the movement with arrows, which are perpendicular to the contours and directed from high values toward those of lower ones (Figure 6.2). The arrows represent the general direction of oil migration.

According to this map, after hydrocarbon generation and expulsion from the thermally mature source rock area, Red River Formation oil migrated/is migrating concentrically toward the edges of the Williston Basin. The central Montana region, characterized by oil heads less than 2500 m, represents a fluid-potential minimum zone developed between opposing migration fields: one is from Wyoming, the other one is from the centre of the basin. This large area is extremely suitable for formation of hydrodynamic traps, but locations of known oil fields and production wells (Figure 4.5) do not confirm this. There could be several reasons for this. First, TDS distribution (Figure 5.1) shows an elongated freshwater tongue deeply intruding into higher salinity areas in south-central Saskatchewan. This meteoric impact, along with the concurrent, possible higher flow rate, might have caused flushing of existing accumulations, or destruction of conditions for potential sites of promising occurrences. Other possible actors could be biodegradation, lack of permeable reservoir rocks, or lack of exploration activity.

6.3.2 Oil Migration in the Red River Formation

The distribution of oil production from the Red River Formation (Figure 4.5) extends beyond the area where source rocks generated oil (Figure 1.1). Solvent extract data from gas chromatograms, vitrinite reflectance profiles, and Rock-Eval results (Osadetz et al., 1992) prove that the Red River Formation reached the sufficient level of maturity to generate oil over limited areas of the basin. To date there is no evidence that hydrocarbons were generated outside this zone. Some of the producing fields are far removed from viable source rocks (e.g., Lantry Field in South Dakota (Longman et al., 1998)). These oils most likely migrated laterally a few 10's, or up to more than 100 km.

Petroleum migration over long distances in North American sedimentary basins is well-documented. Dow (1974) suggested that petroleum in the Williston Basin migrated more than 150 km. Other descriptions of long-range migration include the Denver Basin (Clayton and Swetland, 1980), the Big Horn and Powder River Basins (Sheldon, 1967), the Alberta Basin (Demaison, 1977, Garven, 1989), and the Illinois Basin (Bethke et al., 1991).

Based on maturity versus depth cross-plots, Osadetz et al. (1991) believe that Ordovician sourced oils are characterized by short migration pathways. Fowler et al. (1998) argues that a significant lateral migration distance is implied within the formation. Both studies agree that reserves of Red River oils are sourced from and reservoired in the formation. Migration in the Red River Formation occurred by Late Eocene time, post-dating the formation of the Cedar Creek Anticline, but pre-dating the closure on the Nesson Anticline (Burrus et al., 1995). Therefore, Red River-oils can be found in Cedar Creek pools but they had not been trapped close to the Nesson

Anticline. It suggests that much of the oil migrated to the northeastern flank of the Williston Basin where huge oil resources may be present (ibid.). This idea is supported by the results of the recent investigation.

Magnitudes of hydrodynamic and buoyant forces (Figure 5.12) could drive migration far away from the mature area. The reason why distant fields are not common in the basin is not fully understood. There are a few feasible explanations:

1. Fields do exist, but have not been found yet.
2. Stratigraphic and lithostratigraphic factors made forming of fields impossible.

The efficiency of migration in a carrier bed is greatest when oil flows through only a small fraction of the bed so it is less likely dissipated as irreducible saturation and rapid enough to reach distant traps (England et al., 1987). Significant quantities of oil would be lost and long-range migration impeded if migration occurred in the entire bed. Porosity and grain size maps of the Red River Formation (Maccary et al., 1983; Downey, 1984) show that the mature source rock area is surrounded by a thick, porous zone (dolomite or dolomitic limestone), which could be thick enough (>35 m) to prevent effective migration over long distances.

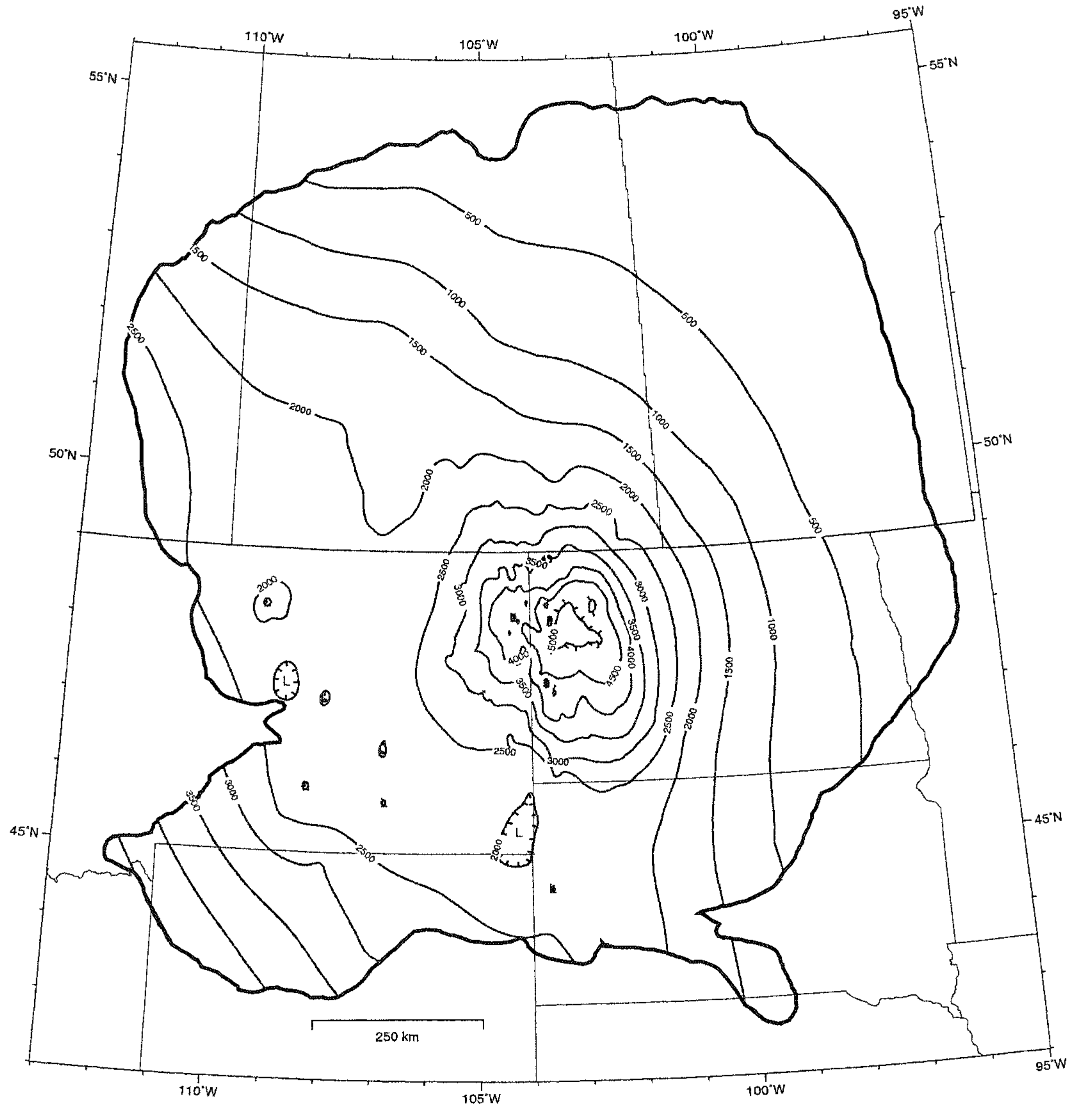

Figure 6.1 Entrapment Potential (UVZ) map (C.I. = 500 m)

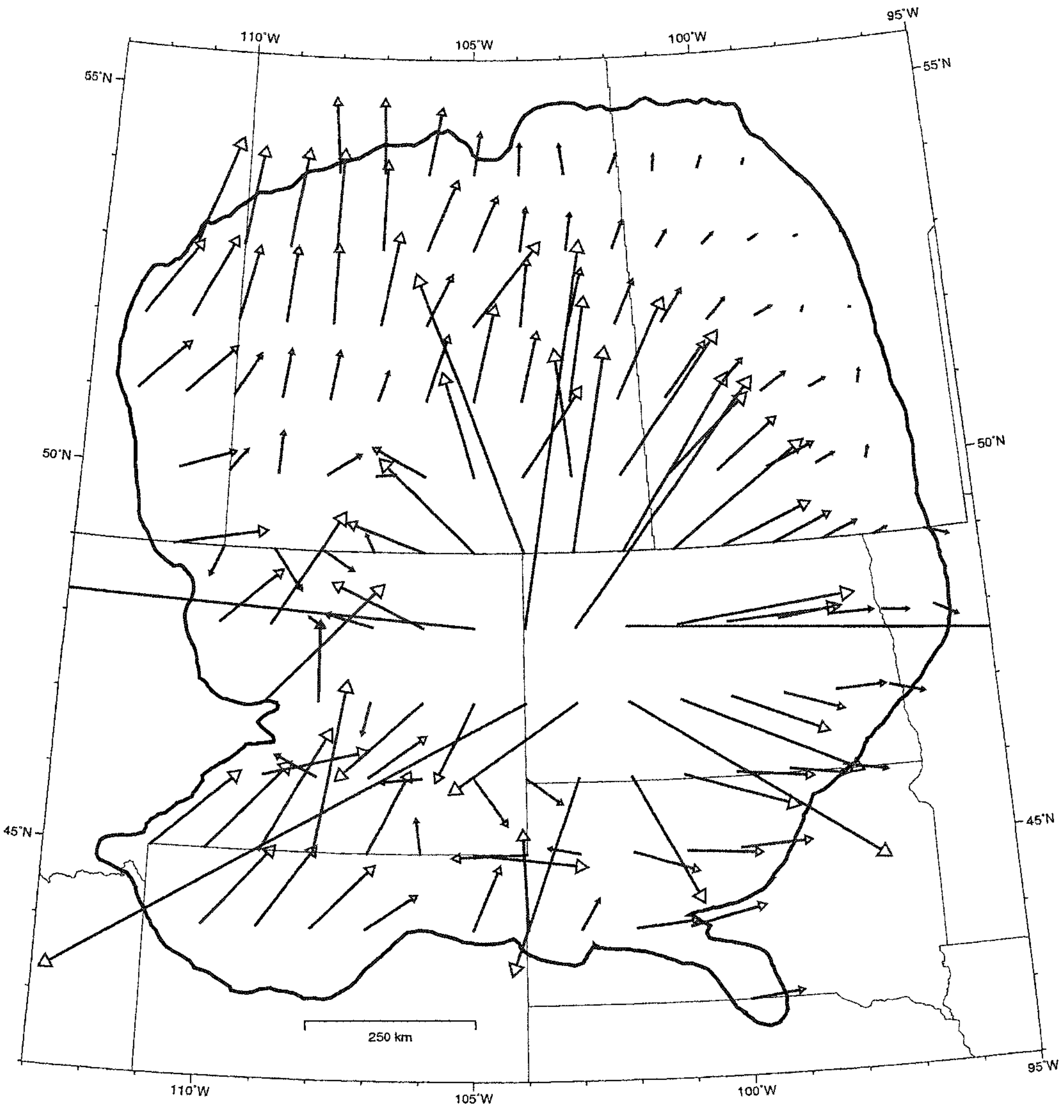

Figure 6.2 Map showing vectors of the density-modified oil heads in the Red River Formation

Chapter 7 - Summary

7.1 Conclusions

1. The Williston Basin spans several political boundaries, thus there is a need to study the basin ignoring these borders. To accomplish that, creation of a database for the Red River Formation was required. The database contains all reasonably available parameters from private and commercial agents, covering most of the study area.

2. There is a wide range in total dissolved solids in the Red River Formation, from a few 10's to more than 400 g/l. The dominant ions are chloride, sodium, and calcium. Three distinctive types represent waters in the Red River Aquifer, which are $CaSO_4$, NaCl, and Na-CaCl. The first water type ($CaSO_4$) occurs where the flow system is active (freshwater tongue, northern part of the study area). TDS, chloride, and sodium are relatively low and unimportant, while calcium and bicarbonate are at an elevated level. The second one (NaCl) is characterized by higher TDS (50-300 g/l). Chloride and sodium-potassium become dominant, calcium is less influential than in the previous type. The third type can be found at the deep part of the formation, with high TDS. Chloride is almost entirely the only anion, and calcium becomes as abundant as sodium.

3. Temperatures showed no observable advective effects at the scale of this investigation.

4. Most oil field areas are characterized by:

- high TDS water (>300 g/l)

- elevated water densities
- slow groundwater flow.

5. Two distinctive flow regimes exist in the Red River Formation: a shallower one, which is gravity driven, and originates from the high elevation mountains, and a sluggish brine body in the deep basin, for which buoyancy effects are important.

6. There is resemblance between hydraulic head distribution and topography. The principal groundwater flow direction is from the highlands to north-, then northeastward, towards the Canadian Shield and eastern North Dakota.

7. Ionic concentrations reflect the direction of groundwater flow from recharge zones towards the central part of the basin. Areas of high total dissolved solids coincide with those of high chloride, sodium, and calcium. The observed freshwater tongue in southern-southwestern Saskatchewan may originate from recharge of the nearby Bearpaw Uplift in northern Montana.

8. Freshwater hydraulic heads have a decreasing trend to north-northeast, but must be modified where high-density waters are present. It appears that three hydrodynamic zones exist. The first one is situated on the western, southwestern portion of the study are, the second one occupies the central part, and the third one is located on the eastern, northeastern, northern segment.

9. Hubbert's UVZ-method has been applied. Although every effort was made to prove or refute the theory, remarkable correspondence between known traps and computed fluid potential minima was not observed. However, hydrocarbon migration patterns were clearly identified. Oils tend to migrate radially outward from the thermally mature source rock area. North of 49° N, the general direction is similar to the groundwater flow directions: north- and northeastward. In the Dakotas, migration

points to the shallower parts of the formation. In Montana, maps reveal opposing migration fields.

7.2 Recommendations

In conclusion, the interpretation and results presented in this thesis are intended to serve as a basis for future studies in relation to the Red River Formation. Among others, basement control on hydrocarbon production, detailed characterization of sedimentation, and calculation of rate of recharge and discharge are proposed as an aid for better understanding of the nature and relationship of groundwater flow and hydrocarbon migration, accumulation and production. Detailed studies on geothermics are recommended to determine the role of groundwater in the distribution of heat patterns. Application of the UVZ-method is encouraged on large-scale maps, combining with the construction of "UVZ cross-sections" to define the relationship between hydrocarbon accumulations and oil potential minima.

References

Andrichuk, J. M., 1959, Ordovician and Silurian Stratigraphy and Sedimentation in Southern Manitoba, Canada: American Association of Petroleum Geologists Bulletin, v. 43, no. 10, p. 2333-2398.

Bachu, S., and Hitchon, B., 1996, Regional-Scale Flow of Formation Waters in the Williston Basin: American Association of Petroleum Geologists Bulletin, v. 80, no. 2, p. 248-264.

Baillie, A. D., 1952, Ordovician Geology of Lake Winnipeg and Adjacent Area, Manitoba: Manitoba Department of Mines and Natural Resources, Mines Branch Publication, 51-6, 64 p.

Barson, D., 1993, The Hydrogeological Characterization of Oil Fields in North-Central Alberta for Exploration Purposes [unpublished Ph.D. thesis]: University of Alberta, 301 p.

Bear, J., 1972, Dynamics of Fluids in Porous Media, Environmental Science Series: New York, Elsevier, 764 p.

Benn, A. A., and Rostron, B. J., 1998, Regional Hydrochemistry of Cambrian to Devonian Aquifers in the Williston Basin, Canada-U.S.A., *in* Eighth International Williston Basin Symposium, Regina, p. 238-246.

Berg, R. R., DeMis, W. D., and Mitsdarffer, A. R., 1994, Hydrodynamic Effects on Mission Canyon (Mississippian) Oil Accumulations, Billings Nose Area, North Dakota: American Association of Petroleum Geologists Bulletin, v. 78, no. 4, p. 501-518.

Bethke, C. M., Reed, J. D., and Oltz, D. F., 1991, Long-Range Migration in the Illinois Basin: American Association of Petroleum Geologists Bulletin, v. 75, no. 5, p. 925-945.

Bezys, R. K., and Conley, G. G., 1998, Manitoba Stratigraphic Database and the Manitoba Stratigraphic Map Series: Manitoba Energy and Mines, Open File Report OF98-7.

Bredehoeft, J. D., Neuzil, C. E., and Milly, P. C. D., 1983, Regional Flow in the Dakota Aquifer: A Study of the Role of Confining Layers, United States Geological Survey Water Supply Paper 2237, 45 p.

Brindle, J. E., 1960, The Faunas of the Lower Paleozoic Carbonate Rocks in the Subsurface of Saskatchewan: Saskatchewan Department of Mineral Resources, 45 p.

Brown, D. L., Blankennagel, R. K., Maccary, L. M., and Peterson, J. A., 1984, Correlation of Paleostructure and Sediment Deposition in the Madison Limestone and Associated Rocks in Parts of Montana, North Dakota, South Dakota, Wyoming, and Nebraska: United States Geological Survey, Professional Paper 1273-B, 24 p.

Burrus, J., Osadetz, K., Wolf, B., Visser, K., and Dearborn, D., 1995, Resolution of Williston Basin Oil System Paradoxes Through Basin Modelling, *in* Seventh International Williston Basin Symposium, p. 235-251.

Burrus, J., Osadetz, K., Wolf, S., Doligez, B., Visser, K., and Dearborn, D., 1996, A Two-Dimensional Regional Basin Model of Williston Basin Hydrocarbon Systems: American Association of Petroleum Geologists Bulletin, v. 80, no. 2, p. 265-291.

Busby, J. F., Kimball, B. A., Downey, J. S., and Peter, K. D., 1995, Geochemistry of Water in Aquifers and Confining Units of the Northern Great Plains in Parts of Montana, North Dakota, South Dakota, and Wyoming: United States Geological Survey, Professional Paper 1402-F, 146 p.

Carroll, K., 1979, Depositional Environments and Paragenetic Porosity Controls, Upper Red River Formation, North Dakota: North Dakota Geological Survey Report of Investigation 66, 51 p.

Cecile, M. P., and Norford, B. S., 1993, Ordovician and Silurian, Subchapter 4C, *in* Sedimentary Cover of the Craton in Canada, Geological Survey of Canada, p. 125-149.

Chebotarev, I. I., 1955a, Metamorphism of Natural Waters in the Crust of Weathering, part 1: Geochimica et Cosmochimica Acta, v. 8, no. 1-4, p. 22-48.

Chebotarev, I. I., 1955b, Metamorphism of Natural Waters in the Crust of Weathering, part 2: Geochimica et Cosmochimica Acta, v. 8, no. 1-4, p. 137-170.

Chebotarev, I. I., 1955c, Metamorphism of Natural Waters in the Crust of Weathering, part 3: Geochimica et Cosmochimica Acta, v. 8, no. 1-4, p. 198-212.

Clayton, J. L., and Swetland, P. J., 1980, Petroleum Generation and Migration in Denver Basin: American Association of Petroleum Geologists Bulletin, v. 64, no. 10, p. 1613-1633.

Collins, A. G., 1975, Geochemistry of Oilfield Waters, Developments in Petroleum Science: Amsterdam, Elsevier Scientific Publishing, 496 p.

Cumming, L. M., 1975, Ordovician Strata of the Hudson Bay Lowlands: Geological Survey of Canada, Paper 74-28, 93 p.

Dachler, R., 1936, Grundwasserströmung: Vienna, J. Springer, 141 p.

Darcy, H., 1856, Determination of the Laws of the Flow of Water Through Sand: Translation in Physical Hydrogeology, Freeze, R.A. and Back, W. (eds.), Hutchinson Ross, New York. Benchmark Papers in Geology 72, p. 14-19.

Darton, N. H., 1905, Preliminary Report on the Geology and Underground Water Resources of the Central Great Plains: United States Geological Survey, Professional Paper 32, 433 p.

Davies, P. B., 1987, Modeling Areal, Variable-Density Groundwater Flow Using Equivalent Freshwater Head - Analysis of Potentially Significant Errors, *in* NWWA/IGWMC, Feb. 10-12, 1987, Denver, Colorado, p. 888-903.

Demaison, G. J., 1977, Tar Sands and Supergiant Oil Fields: American Association of Petroleum Geologists Bulletin, v. 61, no. 11, p. 1950-1961.

Deming, D., and Nunn, J. A., 1991, Numerical Simulation of Brine Migration by Topographically Driven Recharge: Journal of Geophysical Research, v. 96, no. B2, p. 2485-2499.

Dinwiddie, G. A., and Downey, J. S., 1986, Northern Great Plains Regional Aquifer-System Study, *in* Sun, R. J., ed., Regional Aquifer-System Analysis Program, United States Geological Survey, p. 50-71.

Dow, W. G., 1974, Application of Oil-Correlation and Source-Rock Data to Exploration in Williston Basin: American Association of Petroleum Geologists Bulletin, v. 58, no. 7, p. 1253-1262.

Downey, J. S., 1982, Hydrodynamics of the Williston Basin in the Northern Great Plains, *in* C.V. Theis Conferences on Geohydrology, Lincoln, p. 92-98.

Downey, J. S., 1984, Geohydrology and Hydrology of the Madison Limestone and Associated Rocks in Parts of Montana, Nebraska, North Dakota, South Dakota, and Wyoming: United States Geological Survey, 1273-G, 47 p.

Downey, J. S., Busby, J. F., and Dinwiddie, G. A., 1987, Regional Aquifers and Petroleum in the Williston Basin Region of the United States, *in* Williston Basin; anatomy of a cratonic oil province, Denver, p. 299-312.

Downey, J. S., and Dinwiddie, G. A., 1988, The Regional Aquifer System Underlying the Northern Great Plains in Parts of Montana, North Dakota, South Dakota, and Wyoming: United States Geological Survey, Professional Paper, 1402-A, 64 p.

England, W. A., Mackenzie, A. S., Mann, D. M., and Quigley, T. M., 1987, The Movement and Entrapment of Petroleum Fluids in the Subsurface: Journal of the Geological Society, London, v. 144, no. 2, p. 327-347.

Feng, Q., 1997, Modern Hydrogeological Conditions and Oil-Gas Accumulation in Wenjisang, Turpan-Hami Basin: Oil and Gas Geology, v. 18, no. 3, p. 224-227.

Foerste, A. F., 1929, The Cephalopods of the Red River Formation of Southern Manitoba: Bulletin of the Scientific Laboratories of Dension University, v. 29, no. 7, p. 129-235.

Fowler, M. G., Idiz, E., Stasiuk, L. D., Li, M., Obermayer, M., and Osadetz, K.G., 1998, Reexamination of the Red River Petroleum System, Southeastern Saskatchewan, Canada, *in* Eighth International Williston Basin Symposium, Regina, p. 11-13.

Freeze, R. A., and Cherry, J. A., 1979, Groundwater: Englewood Cliffs, Prentice-Hall, 604 p.

Garven, G., 1989, A Hydrogeologic Model for the Formation of the Giant Oil Sands Deposits of the Western Canada Sedimentary Basin: American Journal of Science, v. 289, no. 2, p. 105-166.

Garven, G., and Freeze, R. A., 1984, Theoretical Analysis of the Role of Groundwater Flow in the Genesis of Stratabound Ore Deposits: 1. Mathematical and Numerical Model: American Journal of Science, v. 284, no. 10, p. 1085-1124.

Gerhard, L. C., Anderson, S. B., LeFever, J. A., and Carlson, C. G., 1982, Geological Development, Origin, and Energy Mineral Resources of the Williston Basin, North Dakota: American Association of Petroleum Geologists Bulletin, v. 66, no. 8, p. 989-1020.

Gretener, P. E., 1979, Pore Pressure: Fundamentals, General Ramifications and Implications for Structural Geology, American Association of Petroleum Geologists Education Course Note Series: Oklahoma, American Association of Petroleum Geologists, 131 p.

Gretener, P. E., 1981, Geothermics: Using Temperature in Hydrocarbon Exploration, American Association of Petroleum Geologists Education Course Note Series: Oklahoma, American Association of Petroleum Geologists, 168 p.

Gries, J. P., 1981, Unpublished Maps Prepared for the Office of Drinking Water, South Dakota Department of Water and Natural Resources, for the Underground Injection Control Program: South Dakota Geological Survey.

Gussow, W. C., 1954, Differential Entrapment of Oil and Gas: American Association of Petroleum Geologists Bulletin, v. 38, no. 5, p. 816-853.

Haidl, F. M., 1990, Ordovician Hydrocarbon Reservoirs, Herald and Yeoman Formations (Red River), Southeastern Saskatchewan, Summary of Investigation, Saskatchewan Geological Survey; Saskatchewan Energy and Mines, p. 176-186.

Haidl, F. M., Longman, M. W., Pratt, B. R., and Bernstein, L. W., 1997, Variations in Lithofacies in Upper Ordovician Herald and Yeoman Formations (Red River), North Dakota and Southeastern Saskatchewan, *in* CSPG-SEPM Joint Convention, Core Conference, Calgary, Alberta, p. 5-39.

Hanor, J. S., 1987, Origin and Migration of Subsurface Sedimentary Brines, Society of Economic Paleontologists and Mineralogists, 247 p.

Hermanrud, C., 1986, On the Importance of Petroleum Generation of Heating Effects from Compaction-Derived Water: An Example from the Northern North Sea, *in* Burrus, J., ed., Thermal Modeling of Sedimentary Basins: Paris, Editions Technip, p. 247-269.

Hitchon, B., 1984, Geothermal Gradients, Hydrodynamics, and Hydrocarbon Occurrences, Alberta, Canada: American Association of Petroleum Geologists Bulletin, v. 68, no. 6, p. 713-743.

Hitchon, B., and Brulotte, M., 1994, Culling Criteria for Standard Formation Water Analyses: Applied Geochemistry, v. 9, no. 6, p. 637-645.

Horner, D. R., 1951, Pressure Build-Up in Wells, *in* Third World Petroleum Congress, Proc., Sect. II., Leiden, Holland, p. 503-521.

Hubbert, M. K., 1940, The Theory of Ground-Water Motion: Journal of Geology, v. 48, no. 8, p. 785-944.

Hubbert, M. K., 1953, Entrapment of Petroleum Under Hydrodynamic Conditions: American Association of Petroleum Geologists Bulletin, v. 37, no. 8, p. 1954-2026.

Jankowski, J., and Jacobson, G., 1989, Hydrochemical Evolution of Regional Groundwaters to Playa Brines in Central Australia: Journal of Hydrology, v. 108, no. 1-4, p. 123-173.

Jones, F. W., 1991, The Thermal State of the Williston Basin in Canada, *in* Sixth International Williston Basin Symposium, Regina, p. 216-221.

Judge, A. S., 1973, Deep Temperature Observations in the Canadian North, *in* Permafrost; North American Contribution, Second International Conference, Washington, D.C., p. 35-40.

Kendall, A. C., 1976, The Ordovician Carbonate Succession (Bighorn Group) of Southeastern Saskatchewan: Department of Mineral Resources, Saskatchewan Geological Survey Bulletin 180, 185 p.

Kent, D. M., 1960, The Evaporites of the Upper Ordovician Strata in the Northern Part of the Williston basin: Saskatchewan Department of Mineral Resources, Report 49, 26 p.

Kent, D. M., 1987, Paleotectonic Controls on Sedimentation in the Northern Williston Basin, Saskatchewan, *in* Williston Basin; Anatomy of a Cratonic Oil Province, Denver, p. 45-56.

Kerr, S. D., 1988, Overview: Williston Basin Carbonate Reservoirs: Denver, Rocky Mountain Association of Geologists, 251-274 p.

Kohm, J. A., and Louden, R. O., 1978, Ordovician Red River of Eastern Montana-Western North Dakota: Relationship between Lithofacies and Production, *in* Williston Basin Symposium, 24th Annual Conference, Billings, Montana, p. 99-117.

Kreis, L. K., and Haidl, F. M., 1997, Geology of the Upper Ordovician Red River Strata (Herald and Yeoman Formations); Lower Paleozoic Formations Map Series: Saskatchewan Geological Survey, Sask. Energy Mines, scale 1:2000000.

Kreis, L. K., and Kent, D. M., 2000, Basement Controls on Red River Sedimentation and Hydrocarbon Production in Southeastern Saskatchewan: Saskatchewan

Geological Survey, Saskatchewan Energy Mines, Misc. Rep. 2000-4.1, p. 21-42.

Laird, W. M., 1956, The Williston Basin - A Backward Look with a View to the Future: *in* First International Williston Basin Symposium, Bismarck, North Dakota, p. 14-22

Leenheer, M. J., and Zumberge, J. E., 1987, Correlation and Thermal Maturity of Williston Basin Crude Oils and Bakken Source Rocks Using Terpane Biomarkers, Williston Basin: Anatomy of a Cratonic Oil Province: Denver, Rocky Mountain Association of Geologists, 287-298 p.

LeFever, R. D., 1998, Hydrodynamics of Formation Waters in the North Dakota Williston Basin, *in* Eighth International Williston Basin Symposium, Regina, p. 229-237.

Lepard, D. W., and Nairn, K. N., 1995, TWPGRID and Related Utilities for Township-Range Grids in Western Canada: Geological Survey of Canada, Open File Report 3105.

Li, M., Osadetz, K. G., Fowler, M. G., Snowdon, L. R., Stasiuk, L. D., Yao, H., Hwang, R. J., Jenden, P. D., Grant, B. D., and Idiz, E., 1998a, Case Studies on Secondary Oil Migration in the Williston Basin, *in* Eighth International Williston Basin Symposium, Regina, p. 247-253.

Li, M., Osadetz, K. G., Obermayer, M., Fowler, M. G., Snowdon, L. R., and Christensen, R., 1998b, Organic Geochemical Indications of Post-Devonian Magmatic Intrusions in Southeastern Saskatchewan, *in* Eighth International Williston Basin Symposium, Regina, p. 179-188.

Longman, M. W., Bogle, R., and Single, E. L., 1998, Lantry Field, South Dakota: An Odd Red River Reservoir on the Southeast Flank of the Williston Basin, *in* Eighth International Williston Basin Symposium, Regina, p. 14-23.

Maccary, L. M., Cushing, E. M., and Brown, D. L., 1983, Potentially Favorable Areas for Large-Yield Wells in the Red River Formation and Madison Limestone in Parts of Montana, North Dakota, South Dakota, and Wyoming: United States Geological Survey, Professional Paper, 1273-E, 13 p.

Majorowicz, J. A., Jones, F. W., and Jessop, A. M., 1986, Geothermics of the Williston Basin in Canada in relation to Hydrodynamics and Hydrocarbon Occurrences: Geophysics, v. 51, no. 3, p. 767-779.

Martiniuk, C. D., and Barchyn, D., 1994, Petroleum Potential of the Pre-Mississippian, Southwestern Manitoba: Bulletin of Canadian Petroleum Geology, v. 42, no. 3, p. 365-391.

Martiniuk, C. D., Young, H. R., and Klassen, H. J., 1998, Regional Overview of the Geology and Petroleum Potential, Red River Formation, Southwestern Manitoba, Manitoba Energy and Mines, 41 p.

McCabe, H. R., and Bannatyne, B. B., 1970, Lake St. Martin Crypto-Explosion Crater and Geology of the Surrounding Area: Winnipeg, Manitoba, Manitoba Department of Mines and Natural Resources, 79 p.

Meinzer, O. E., 1923, Outline of Groundwater Hydrology - With Definitions, United States Geological Survey Water Supply Paper 494, 71 p.

Meissner, F. F., and Banks, R. B., 2000, Computer Simulation of Hydrocarbon Generation Migration and Accumulation under Hydrodynamic Conditions - Examples from the Williston and San Juan Basins, USA, *in* American Association of Petroleum Geologists International Conference and Exhibition, Bali, Indonesia.

Meyer, M., 1984, Evaluation of the Groundwater Resources of Western South Dakota, Task 5: Water Quality Suitability by Aquifer for Drinking, Irrigation, Livestock Watering and Industrial Use., U.S. Army Corps of Engineers, 200 p.

Minerals Diversified Services, Inc., 1998, Manual to Accompany: Williston Basin Oil and Gas Fields Map with Cumulative Production by Pool. Dakotas, Montana, Manitoba, Saskatchewan, 38 p.

Montgomery, S. L., 1997, Ordovician Red River 'B' - Horizontal Oil Play in the Southern Williston Basin: American Association of Petroleum Geologists Bulletin, v. 81, no. 4, p. 519-532.

Mossop, G. D., and Shetsen, I., 1994, Geological Atlas of the Western Canada Sedimentary Basin: Calgary, Canadian Society of Petroleum Geologists and Alberta Research Council, 510 p.

Munn, M. J., 1909, The Anticlinal and Hydraulic Theories of Oil and Gas Accumulation: Economic Geology, v. 4, no. 6, p. 509-529.

Murray, G. H., 1959, Examples of Hydrodynamics in the Williston Basin at Poplar and North Tioga Fields, American Association of Petroleum Geologists Rocky Mtn. Sec., Geological record, p. 55-59.

Muskat, M., 1937, Flow of Homogeneous Fluids Through Porous Media: I.H.R.D.C. Publications, Boston, Massachusetts, 763 p.

Neuzil, C. E., Bredehoeft, J. D., and Wolff, R. G., 1982, Leakage and Fracture Permeability in the Cretaceous Shales Confining the Dakota Aquifer in South Dakota, *in* C.V. Theis Conferences on Geohydrology, p. 113-120.

Obermayer, M., Osadetz, K. G., and Snowdon, L. R., 1998, Familial Association and Sources of Oil Quality Variation in the Williston Basin from Gasoline Range and Saturated Hydrocarbon Parameters, *in* Eighth International Williston Basin Symposium, Regina, p. 209-225.

Osadetz, K. G., Brooks, P. W., and Snowdon, L. R., 1992, Oil Families and Their Sources in Canadian Williston Basin (southeastern Saskatchewan and southwestern Manitoba): Bulletin of Canadian Petroleum Geology, v. 40, no. 3, p. 254-273.

Osadetz, K. G., Kohn, B. P., O'Sullivan, P., Feinstein, S., Hannigan, P. K., Everitt, R. A., Gilboy, C. F., Bezys, R. K., and Stasiuk, L. D., 1998, Williston Basin Thermotectonics: Variations in Heat Flow and Hydrocarbon Generation, *in* Eighth International Williston Basin Symposium, Regina, p. 147-165.

Osadetz, K. G., and Snowdon, L. R., 1995, Significant Paleozoic Petroleum Source Rocks in the Canadian Williston Basin: Their Distribution, Richness and Thermal Maturity (Southeastern Saskatchewan and Southwestern Manitoba): Geological Survey of Canada Bulletin 487, 60 p.

Osadetz, K. G., Snowdon, L. R., and Brooks, P. W., 1991, Relationships Amongst Oil Quality, Thermal Maturity and Post-Accumulation Alteration in Canadian Williston Basin (Southeastern Saskatchewan and Southwestern Manitoba), *in* Sixth International Williston Basin Symposium, Regina, p. 293-311.

Paul, D., 1994, Hydrogeology of the Devonian Rimbey-Meadowbrook Reef Trend of Central Alberta [unpublished M.Sc. thesis]: University of Alberta, 152 p.

Piper, A. M., 1944, A Graphic Procedure in the Geochemical Interpretation of Water Analyses: Trans. American Geophysical Union, v. 25, p. 914-923.

Porter, J. W., and Fuller, J. G. C. M., 1959, Lower Paleozoic Rocks of Northern Williston Basin: American Association of Petroleum Geologists Bulletin, v. 43, no. 1, p. 124-189.

Potter, D., and St. Onge, A., 1991, Minton pool, South-Central Saskatchewan: A Model for Basement Induced Structural and Stratigraphic Relationships, *in* Sixth International Williston Basin Symposium, Regina, p. 21-33.

Powley, D. E., 1990, Pressures and Hydrogeology in Petroleum Basins: Earth-Science Reviews, v. 29, p. 215-226.

Rakhit Petroleum Consulting Limited, R., 1999, Hydrogeology of the Williston Basin, Phase III.3.Present and Paleo Oil Migration Patterns; Ordovician Petroleum Systems.

Rédly, P., 1998, Tectonostratigraphic Evolution of the Williston Basin [unpublished Ph.D. thesis]: University of Saskatchewan, 360 p.

Rich, J. L., 1921, Moving Underground Water as a Primary Cause of the Migration and Accumulation of Oil and Gas: Economic Geology, v. 16, no. 6, p. 347-371.

Rostron, B., 1994, A New Method for Culling Pressure Data Used in Hydrodynamic Studies, American Association of Petroleum Geologists Annual Convention Volume: Denver, American Association of Petroleum Geologists and Society of Economic Paleontologists and Mineralogists, p. 247.

Rostron, B. J., Holmden, C., and Kreis, L. K., 1998, Hydrogen and Oxygen Isotope Compositions of Cambrian to Devonian Formation Waters, Midale Area, Saskatchewan, *in* Eighth International Williston Basin Symposium, Regina, p. 267-273.

Schowalter, T. T., 1979, Mechanics of Secondary Hydrocarbon Migration and Entrapment: American Association of Petroleum Geologists Bulletin, v. 63, no. 5, p. 723-760.

Shaw, E. W., 1917, Discussion - The Absence of Water in Certain Sandstones of the Appalachian Oil Fields: Economic Geology, v. 12, p. 610-628.

Sheldon, R. P., 1967, Long-Distance Migration of Oil in Wyoming: Mountain Geologist, v. 4, p. 53-65.

Silverman, S. R., 1965, Migration and Segregation of Oil and Gas: *in* Fluids in Subsurface Environments, American Association of Petroleum Geologists Memoir 4, p. 53-65.

Slichter, C. S., 1897-1898, Theoretical Investigations of the Motion of Ground Waters: U.S. Geological Survey 19th Annual Report, p. 294-384.

Tissot, B. P., and Welte, D. H., 1978, Petroleum Formation and Occurrance: New York, Springer Verlag, 699 p.

Tóth, J., 1978, Gravity-Induced Cross-Formational Flow of Formation Fluids, Red Earth Region, Alberta, Canada: Analysis, Patterns and Evolution: Water Resources Research, v. 14, no. 5, p. 805-843.

Tóth, J., 1980, Cross-formational Gravity-flow of Groundwater: A Mechanism of the Transport and Accumulation of Petroleum (The Generalized Hydraulic Theory of Petroleum Migration), *in* Roberts III, W. H., and Cordell, R. J., eds., Problems of Petroleum Migration, American Association of Petroleum Geologists, p. 121-169.

Tóth, J., 1984, The Role of Regional Gravity Flow in the Chemical and Thermal Evolution of Ground Water, *in* First Canadian /American Conference on Hydrogeology, p 3-39.

Tóth, J., and Corbet, T., 1986, Post-Paleocene Evolution of Regional Groundwater Flow-systems and Their Relation to Petroleum Accumulations, Taber Area, Southern Alberta, Canada: Bulletin of Canadian Petroleum Geology, v. 34, no. 3, p. 339-363.

Wefald, M., 1995, Unpublished Coordinate Conversion Utility: .

Wessel, P., and Smith, W. H. F., 1991, Free Software Helps Map and Display Data: EOS Transactions, American Geophysical Union, v. 72, no. 41, p. 445-446.

Wessel, P., and Smith, W. H. F., 1995, New Version of the Generic Mapping Tools Released, EOS Transactions, American Geophysical Union, p. 329.

Wilkinson, P. K., 1995, Is Fluid Flow in Paleozoic Formations of West Central Alberta Affected by the Rocky Mountain Thrust Belt? [unpublished M.Sc. thesis]: University of Alberta, 102 p.

Williams, J. A., 1974, Characterization of Oil Types in Williston Basin: American Association of Petroleum Geologists Bulletin, v. 58, no. 7, p. 1243-1252.

Zawisza, L., 1986, Hydrodynamic Conditions of Hydrocarbon Accumulation Exemplified by the Carboniferous Formation in the Lublin Syclinorium, Poland: Society of Petroleum Engineers Formation Evaluation, v. 1, no. 3, p. 286-294

Appendix A

Data used in the thesis can be found on a CD.